Sudan University of Sciences& Technology

College of Graduated Studies

Verification of Head and Neck External Beam Irradiation in Radiation Therapy

التحقق من حزمة الشعاع الخارجي للرأس والعنق في العلاج الإشعاعي

A thesis submitted for fulfillment of M.Sc. Degree in Radiation Therapy

By:

Shahnaz Idris Bakheet Khalifah

Supervisor:

Dr. MOHAMED ELFADIL MOHAMED GARALNABY

2017

بسم الله الرحمن الرحيم

قال تعالى:

(31) وعلم آدم الأسماء كلها ثم عرضهم على الملائكة فقال أنبئوني بأسماء هؤلاء إن كنتم صادقين قالوا سبحانك لا علم لنا إلا ما علمتنا إنك أنت العليم الحكيم(32)

صدق الله العظيم

سورة البقره

Dedication

This thesis is dedicated to:

My lovely parents

My Brothers and Sisters

Dear MUTAZ

My Friends

Acknowledgment

My acknowledgment and gratefulness at the beginning is to God who gives me the gift of mind.

Profound thanks and gratitude to everyone encouraged and supported me to complete this research.

My gratitude to my supervisor

Dr\MOHMED ALFADIL

In addition, my special thanks, deep gratitude and appreciation extended to my family, friends and my fiancée who stood beside me at every moment. At the end my gratitude is to everyone helped me.

Abstract

The role of verification is primarily to detect treatment delivery errors and secondly, to assess the suitability of the size of the margins planned around the clinical target volume that allow for the uncertainties in the radiotherapy process. This study that was performed in RICK including 57 patients, 30 of them were female represented (52.6%) and 27 were male represented (47.4%), aimd to verify the geometrical and dosemetric changes during external radiation therapy of brain, nasopharynx and maxillary antrum cancer. The data was collected from the patient's records, simulation process and treatment by using master data sheet and simulator images in addition to treatment portal films. Using Interactive Data Language IDL software to measure the dimension and length of each axis for all images. Moreover, the results showed that the mean of simulator in X-axis 9.68±4.64 and for treatment film X-axis was 9.64±4.52, and for Y-axis for simulator 9±3.45 and for treatment film 8.96±3.25. Using paired sample t-test show there is no significant differences between simulator and treatment film for X-axis and between simulator and treatment film for Y-axis.

The association between simulator and treatment film for X-axis was 0.96 mm/mm, and for Y-axis was 0.94 mm/mm.

Linear regression results showed that the rate of association for the simulator (X-Axis) and Treatment film (X-Axis) increases by 0.313 mm, and the rate of association between simulator (Y-Axis) and Treatment film (Y-Axis) increases by 0.437 mm.

A linear correlation was represented between treated and simulated collimator rotation, were the correlation was very strong according to $R^2=0.9998$. In addition, another inverse relation was found between total dose and source collimator rotation, the TD is decreased by 0.063Gry pear each degree of the collimator.

الخلاصه:

الدور الأساسي للتحقق في العلاج بالأشعه هو اولا لإكتشاف الأخطاء في تلقي العلاج ’ و ثانيا لتقييم مناسبة المساحه حول الحجم المستهدف والذي يسمح للأخطاء غير المتوقعه في عمليه العلاج بالأشعه.هدفت هذه الدراسه التي أجريت في مركز الخرطوم للعلاج بالأشعه والطب النووي مشتمله على 57مريض 30 انثى بنسبة 52.6 % و27 ذكر بنسبة47.4% للتحقق من التغيرات الممكن حدوثها في القياسات والجرع أثناء العلاج بالأشعه لسرطان المخ- البلعوم الأنفي والفك العلوي. جمعت المعلومات من التقارير الطبيه للمرضى-صور التخطيط أثناء عملية المحاكاه بجهاز التخطيط –بالإضافه للصور المأخوذه أثناء جلسات العلاج خلال الأسبوع الأول من بدأية الجلسات . باستخدام برنامج ال أي دي ال لقياس الأبعاد و الأطوال لكلا المحورين في كل الصور. أظهرت النتيجه أن الوسط للمحور السيني كان8 9.6±4.64 و 9.64 ±4.52 للتخطيط والعلاج على التوالي، أما بالنسبه للمحور الصادي 9±3.45 على التتابع .أستعمال أختبار ألأزواج المقترنه أظهر أنه لا توجد اختلافات مؤثره بين أفلام التخطيط والعلاج في كلا المحوريين السيني والصادي معا.التغيير في المحور السيني كان 0.96 ملم ، و للمحور الصادي 0.94 ملم .النتيجه أظهرت أن معدل الزياده الخطية في المحور السيني للتخطيط والعلاج على التوالي كانت 0.313 ملم ،أما بالنسبه للمحور الصادي فكانت 0.437 ملم للتخطيط والعلاج بالترتيب . لاحظنا تغيرا في قيم المحور السيني والصادي للسميوليتر و فلم العلاج معا في علاقه طرديه .

بالإضافه لذلك وجدنا أن علاقه خطيه قوية جدا بين زاوية دوران الحقل الإشعاعي بالنسبه للتخطيط والعلاج وذلك ماتثبته المعادله التاليه ر٢= 0.9998 ،بحيث تتناسب هذه العلاقه عكسيا زيادة أو نقصانا مع الجرعه الواصله للأعضاء شديدة الحساسيه للإشعاع بواقع 0.063 جراي لكل درجه.

List of contents

List of figures

List of tables

Chapter one

Introduction

1-1 Incidence of heah and neck cancer:

Greenlee et al. (2001), the most frequent malignant head and neck neoplasms can be grouped under two major headings. The most abundant are the epithelial malignancies of the mucous membranes of the upper aerodigestive tract, so-called head and neck squamous cell carcinoma (HNSCC), accounting for about 90% of all head and neck neoplasms.

Parkin et al. (1999), the second largest group of neoplasms can be described as “glandular neoplasms”, the majority arising in the thyroid, a minority in the salivary glands. Skin cancer is generally considered a separate entity, and so is skin cancer of the head and neck, mainly including squamous cell carcinoma and basal cell carcinoma. Less frequent head and neck neoplasia includes localized lymphoma, soft tissue and bone tumors (sarcomas), and neuroectodermal tissue tumors (paraganglioma, olfactory neuroblastoma, neuroendocrine carcinoma, malignant melanoma).Head and neck cancer, exclauding skin cancer and Hodgkin and non-Hodgkin lymphoma, is the sixth most frequent cancer worldwide.

Radiotherapy treats cancer by using high-energy rays to destroy the cancer cells, while doing as little harm as possible to normal cells. It’s an important treatment for head and

neck cancers. Radiotherapy can be used on its own but is often given in combination with chemotherapy (called chemoradiation).

Radiotherapy may be given:

- After surgery (with or without chemotherapy) to destroy any remaining cancer and reduce the risk of cancer coming back.
- In combination with chemotherapy (chemoradiation), without surgery.
- In combination with the targeted therapy drug.
- To reduce symptoms caused by a tumour (palliative radiotherapy).

Chemoradiation:

Chemoradiation is often the main treatment for advanced head and neck cancers. It may be used:

- To treat cancers that can't be removed with an operation
- To treat cancers in harder-to-reach areas such as the nasopharynx or throat.
- When surgery could cause unacceptable changes to speech or swallowing.

1-2 Problem of study:

Treatment verification is an important component of radiotherapy. The role of verification is primarily to detect treatment delivery errors and secondly, to assess the suitability of the size of the margins planned around the clinical target volume that allow for the

uncertainties in the radiotherapy process. The treatment of Head and Neck cancer with Conventional external beam radiation therapy includes significant radiation to be delivered to the tumor, bed of tumor because of radioresistane aspect of some tissues, and the dose delivered to the organs at risk**.** While treatment verification is an important chateractstic in EBRT of the patients with brain, nasopharynx and maxillary antrum cancer because of possible treatment dosemetric and geometric changes that may occur during the session due to the patient setup errors which can affect the critical healthy structures surrounding the tumor and possible radiated dose to the tumors which should be enclosed with 95% of prescribed dose that make evaluation of this variations is necessary step. So, this study focused on verification of dosemetric and geometric deviations that may occur during the treatment sessions and possible effective dose to tumors and OAR using stimulator and portal images.

1-3 Objectives of the Study:

1-3-1 General Objective:

- The general objective of this study was to verify the geometrical and dosemetric changes during external radiation therapy of brain, nasopharynx and maxillary antrum

cancer, with determination of the accuracy of planning and treatment according to this change.

1-3-2 Specific Objectives:

- To evaluate the geometric changes in external radiation therapy of brain, nasopharynx and maxillary antrum tumors using portal film.
- To calculate the dose changes.
- To correlate between between TD and SSD, present pathologic staging and grade.
- To determine the accuracy of the planning and treatment matching.

Significant of the study:

- The study was focus on verification of geometric and dosemetric changes during EBRT of brain, nasopharynx and maxillary antrum and determine the accuracy of the planning and treatment according to this changes, parameters was modify in acceptable level to guarantees delivery of prescribed dose to tumors and little amount of errors.

1-4 Overview of the study:

This study consisted of five chapters, with chapter one is an introduction introduce briefly this thesis and is contain (anatomy, techniques used for treatment, problem of study also

contain general, specific objectives and significant of study). Chapter two included literature reviews previous studies about the brain, nasopharynx and maxillary antrum external irradiation field verification. Chapter three described the exact methodology (material, method) used. Chapter four includes result presentation and finally chapter five contains the discussion, conclusion and recommendations for future scope in addition to references and appendices.

Chapter Tow

Background and Literature review

2-1 Anatomy:

2-1-1 Brain:

The brain is a spongy organ made up of nerve and supportive tissues. It is located in the head and is protected by a bony covering called the skull. The base, or lower part, of the brain is connected to the spinal cord. Together, the brain and spinal cord are known as the central nervous system (CNS). The spinal cord contains nerves that send information to and from the brain. The CNS works with the peripheral nervous system (PNS). The PNS is made up of nerves that branch out from the spinal cord to relay messages from the brain to different parts of the body. Together, the CNS and PNS allow a person to walk, talk, and throw a ball and so on. The brain has 3 main parts: cerebrum, cerebellum and brain stem (Martini et al, 2012).

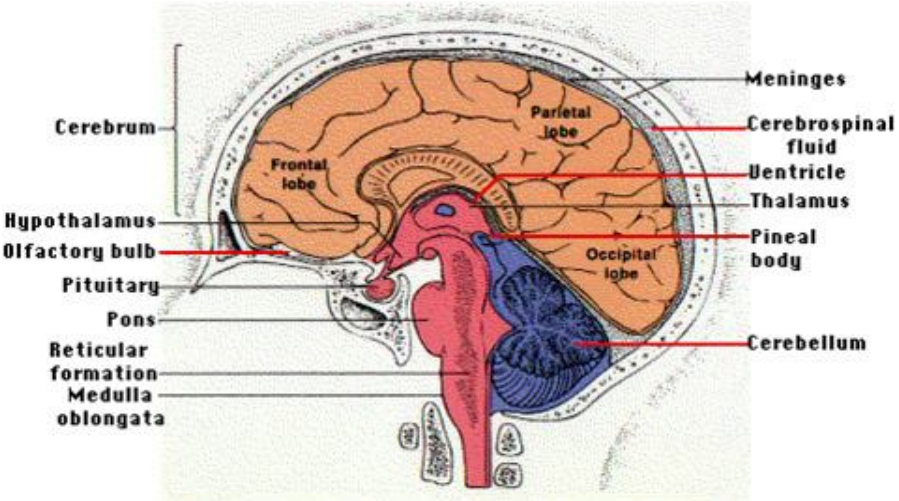

2-1-2 Nasopharynx:

The nasopharynx is a non-collapsible tube, sited above the soft palate and posterior to the nasal cavity. The roof of the nasopharynx curves inferiorly as it progresses posteriorly, and is continuous with the posterior wall of the oropharynx. The anterior aspect is formed by the body of the sphenoid bone, and the curved posterior aspect by the basilar part of the occipital bone. The most postero-inferior part of the nasopharynx is separated from the anterior arch of the atlas by the pharyngobasilar fascia and the superior constrictor muscle. The roof contains the pharyngeal tonsil (adenoid). The lateral walls of the nasopharynx contain the opening of the pharyngotympanic tube. The cartilage of this tube causes the mucosa to bulge, forming the tubal elevation. The tubal tonsil lies just posterior to the elevation, and two folds (the salpingopharyngeal and more anterior salpingopalatine folds) pass inferiorly from the tubal elevation to the pharynx and soft palate respectively. Behind the tonsil the tubal tonsil is the pharyngeal recess. The floor of the nasopharynx formed by the nasal surface of the soft palate. The floor is the only mobile part of the nasopharynx. The nasopharynx communicates with the nasal cavity through the paired nasal apertures, and with the oropharynx through the pharyngeal isthmus(Martini et al, 2012).

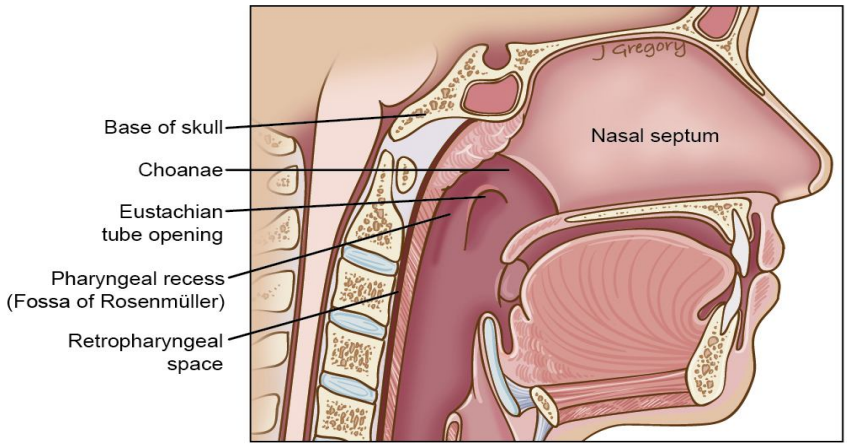

2-1-3 Maxilla:

The maxillary sinus is one of the four paranasal sinuses, which are sinuses located near the nose. The maxillary sinus is the largest of the paranasal sinuses. The two maxillary sinuses are located below the cheeks, above the teeth and on the sides of the nose. The maxillary sinuses are shaped like a pyramid and each contain three cavities, which point sideways, inwards, and downwards. The sinuses are small air-filled holes found in the bones of the face. They reduce skull weight, produce mucus, and affect the tone quality of a person's voice. The maxillary sinus drains into the nose through a hole called the ostia. When the ostia becomes clogged, sinusitis can occur. The ostia of the maxillary sinus often clog because the ostia are located near the top of the maxillary sinus, thus making proper drainage difficult. Maxillary sinusitis or an infection of the maxillary sinus can have the following symptoms: fever, pain or pressure in face near the cheekbones, toothache, and runny nose. Sinusitis is the most common of maxillary sinus illnesses and is usually treated with prescription antibiotics (Martini et al, 2012).

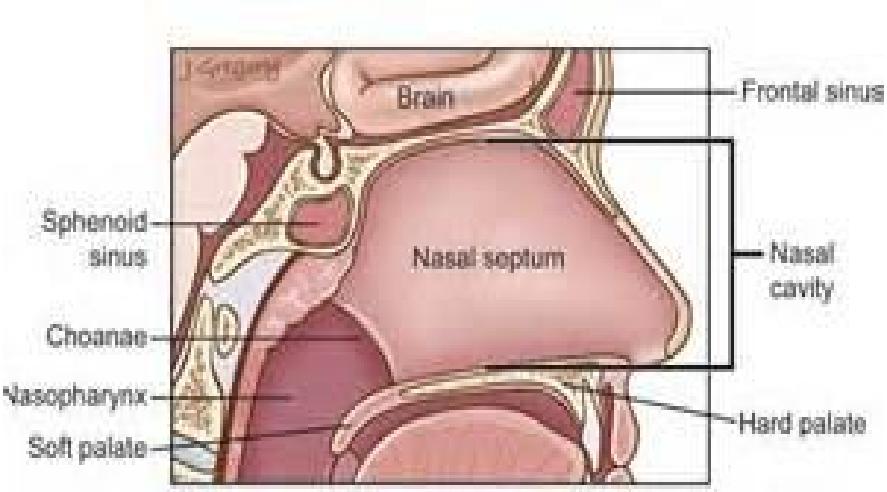

2-2 Literature review

Ballivy et al. (2006) they assessed the effect of geometric uncertainties on target coverage and on dose to the organs at risk (oars) during intensity-modulated radiotherapy (imrt) for head-and-neck cancer, and they estimated the required margins for the planning target volume (ptv) and the planning organ-at-risk volume (prv). For eight head-and-neck cancer patients, they generated imrt plans with localization uncertainty margins of 0 mm, 2.5 mm, and 5.0 mm. The beam intensities were then applied on repeat computed tomography (ct) scans obtained weekly during treatment, and dose distributions were recalculated. The dose–volume histogram analysis for the repeat ct scans showed that target coverage was adequate ($V_{100} \geq 95\%$) for only 12.5% of the gross tumour volumes, 54.3% of the upper-neck clinical target volumes (ctvs), and 27.4% of the lower-neck ctvs when no margins were added for ptv. The use of 2.5-mm and 5.0-mm margins significantly improved target

coverage, but the mean dose to the contralateral parotid increased from 25.9 Gy to 29.2 Gy. Maximum dose to the spinal cord was above limit in 57.7%, 34.6%, and 15.4% of cases when 0-mm, 2.5-mm, and 5.0-mm margins (respectively) were used for prv. Significant deviations from the prescribed dose can occur during imrt treatment delivery for head-and-neck cancer. Accounting for geometric uncertainties is an important issue with imrt, because the isodose lines conform tightly to the target volume. One approach to compensate for set-up errors, organ motion, and changes in target geometry consists of defining planning target volumes (ptv) for targets and planning organ-at-risk volumes (prv) for critical structures, as recommended by the International Commission on Radiation Units and Measurements (icru) . During treatment, portal imaging can be used to assess the accuracy of field alignment. Thus, set-up verification for imrt usually consists of acquiring orthogonal images to check the isocentre localization. Verification methods that rely on this kind of two-dimensional imaging may not provide a comprehensive overview of all the geometric variations that can influence dose distribution in an imrt treatment. Slight variations in the patient's neck and shoulder positioning may not be properly assessed, and some significant changes in shape because of a patient's weight loss or tumour shrinkage may not be detected. As compared with conventional portal images, ct scan imaging for treatment verification provides a more accurate representation of the geometric variations that occur during a course of head-and-neck imrt, including uncertainties in patient position, isocentre localization, organ motion, and changes in external contour because of

weight loss or tumour shrinkage. The results also show that, for patients treated with comprehensive nodal imrt, errors in shoulder repositioning can cause significant dose perturbations in the lower neck region despite the use of 5.0-mm ptv margins. The use of a thermoplastic mask extending down to the level of the shoulder should be considered in these patients to improve set-up reproducibility.

Stratford et al. (2004) this study aimed to provide evidence-based guidelines for implementing geometric verification into clinical practice provide guidance for each radiotherapy centre to create local management structures, processes and protocols that would aid the implementation of geometric verification practices. This includes describing methods by which each centre can determine: The local verification protocols required, Site-specific and individual patient systematic and random set-up errors, which can be used in defining treatment planning margins. By this process the accuracy of radiotherapy is assessed, by comparing images (or data) of the treatment delivered with that planned. This will use information from either 2D or 3D systems to give different degrees of translational and rotational set-up accuracy data. The term ‘set-up error’ is used to describe the discrepancy between intended and actual treatment position. It comprises a systematic and random component. It is normally calculated as a shift in treatment field position when a treatment image is compared against its corresponding reference. The set-up error may be determined relative to the isocentre, the field borders or both and can contain translational and rotational information. **Systematic error:** is a deviation that occurs in the same

direction and is of a similar magnitude for each fraction throughout the treatment course. It is calculated as the standard deviation (SD) of the distribution of mean errors for each individual patient and is usually given the capital sigma symbol Σ where the subscript 'error' refers to the particular error considered (for example, Σ for the measured systematic set-up error).Systematic errors may be introduced into a patient's treatment at the localization, planning or treatment delivery phases. For this reason, these types of errors are often referred to as treatment preparation errors. **Random error:** is a deviation that can vary in direction and magnitude for each delivered treatment fraction. The set-up error measured from a single image will contain both systematic and random components.

PARKER et al. They stated that external photon beam radiotherapy is usually carried out with more than one radiation beam in order to achieve a uniform dose distribution inside the target volume and an as low as possible a dose in healthy tissues surrounding the target. ICRU Report No. 50 recommends target dose uniformity within +7% and –5% of the dose delivered to a well defined prescription point within the target. Modern photon beam radiotherapy is carried out with a variety of beam energies and field sizes under one of two set-up conventions: a constant source to surface distance (SSD) for all beams or an isocentric set-up with a constant source to axis distance (SAD).In an SSD set-up, the distance from the source to the surface of the patient is kept constant for all beams, while for an SAD set-up the centre of the target volume is placed at the machine

isocentre.Clinical photon beam energies range from superficial (30–80 kVp), through orthovoltage (100–300 kVp), to megavoltage energies (60Co–25 MV).Field sizes range from small circular fields used in radiosurgery, through standard rectangular and irregular fields, to very large fields used for total body irradiation (TBI).Volume definition is a prerequisite for meaningful 3-D treatment planning and for accurate dose reporting. ICRU Reports No. 50 and 62 define and describe several target and critical structure volumes that aid in the treatment planning process and that provide a basis for comparison of treatment outcomes.

Cho et al. They employing advanced computer technology to produce treatment delivery systems capable of precise shaping of dose distributions via computer-controlled multileaf collimators and beam intensity modulation in the modern medical accelerator. It is not always obvious or intuitive to determine the relative position of critical structures and the target volume. The beam's eye view (BEV) is commonly used to visualize the position of target volume and organs at risk (OAR) and to design the parameters of the beam irradiation. In 3D treatment planning, oblique non-coplanar beams can be used. This gives rise to many more possible beam arrangements, making the selection of the optimum treatment technique a complex process. The concept of target eye view (TEV) was introduced as an extension of BEV .The TEV map is constructed by inspecting all possible gantry and table angle rotations, for all possible combinations. The aim of a TEV map is to aid localization and visualization of the geometrically most optimum field positions for the

irradiation of the tumor. The best field positions will ideally not include any OAR that is directly intersected by the beam. Previous investigators used as measure of beam feasibility an approximation of the volume intersection between beams and OARs. Refined this concept by considering the average dose inside the OAR. This is the dose that is computed on a set of sampling points within the organ, using a simple dose computation model. (McShan et al) Improved the intersection approximation method by projecting the structures on a plane perpendicular to the beam direction and then inspecting the overlap between outlines of OARs and PTV. The optimization of beam directions implies adjustment of the field size for every stationary field, including determination of shielding or field forming by a multileaf collimator.

Varatharaj et al. (2010) they confirmed that the evaluation of the agreement between measured and calculated dose plays an essential role in the quality assurance (QA) procedures of intensity-modulated radiation therapy (IMRT). Hear they aimed to compare performances of the two dosemetric systems (EDR2 and I'matriXX) in the verification of the dose distributions calculated by the TPS for brain and head and neck dynamic IMRT cases. The comparison of cumulative fluence by using Kodak extended dose rate (EDR2) and I'matriXX detectors has been done for the evaluation of 10 brain, 10 head and neck IMRT cases treated with 6 MV beams. The parameter used to assess the quality of dose calculation is the gamma-index (g -index) method. The acceptance limits for g calculation we have used are 3% and 3 mm respectively for dose agreement and distance to agreement

parameters. Statistical analyses were performed by using the paired, two-tailed Student t-test, and P< 0.01 is kept as a threshold for the significance level. The qualitative dose distribution comparison was performed using composite dose distribution in the measurement plane and profiles along various axes for TPS vs. EDR2 film and TPS Vs I'matriXX. The quantitative analysis between the calculated and measured dose distribution was evaluated using DTA and g-index. The percentage of pixels matching with the set DTA and g values are comparable for both with EDR2 film and I'matriXX array detectors. Statistically there was no significant variation observed between EDR2 film and I'matriXX in terms of the mean percentage of pixel passing g for brain cases (98.77 +/- 1.03 vs. 97.62 +/- 1.66, P = 0.0218) and for head and neck cases (97.39 +/- 2.13 vs. 97.17 +/- 1.52%, P = 0.7404).

Huizenga et al. (1988) they performed this prospective study to determine the accuracy of radiation field alignment for a group of 22 patients with tumors in the head and neck. The accuracy was assessed by an analysis of 138 megavolt portal films in comparison to 55 simulation films. The distance (at the patient midplane) between corresponding points at the field edges on verification film and simulation film appeared to be 5 mm on the average and the standard deviation 5 mm. The analysis was extended by translational and rotational matching of the fields in order to separate each error in a translation error of the field with respect to the patient and an error in field size or shape. Translation errors appear to be somewhat larger than field size or shape errors. From an analysis of a series of

megavolt films taken every third radiotherapy session, it was concluded that treatment-to-treatment variations are as large as the errors due to the transition from simulation to treatment situation. Further analysis showed that variation of the patient's position within the cast is clearly one of the error sources.

Hess et al. (1995) they verify the deviations between simulation and first check films were quantitatively assessed for 95 unselected head and neck cancer patients. All measured deviations — calculated on the basis of a total of 190 simulation and 380 verification films — were normally distributed, with mean values of 0–3 mm and standard deviations of 3–5 mm. Of the absolute deviations, 50% and 95% were within 3 mm and 9 mm, respectively. These results should be considered in clinical practice when prescribing safety margins and adequate cut off doses for sparing critical organs in head and neck cancer.

Yin et al. (1998) they performed this study to investigate a method for the generation of digitally reconstructed radiographs directly from MR images (DRR-MRI) to guide a computerized portal verification procedure. Several major steps were developed to perform an MR image-guided portal verification procedure. Initially, a wavelet-based multiresolution adaptive thresholding method was used to segment the skin slice-by-slice in MR brain axial images. Some selected anatomical structures, such as target volume and critical organs, were then manually identified and were reassigned to relatively higher intensities. Interslice information was interpolated with a directional method to achieve

comparable display resolution in three dimensions. A Chamfer matching technique was used to correlate features between DRR-MRI and portal image. The MR image-guided portal verification method was evaluated using a brain phantom case and a clinical patient case. Both DRR-CT and DRR-MRI were generated using CT and MR phantom images with the same beam orientation and then compared. The matching result indicated that the maximum deviation of internal structures was less than 1 mm. The segmented results for brain MR slice images indicated that a wavelet-based image segmentation technique provided a reasonable estimation for the brain skin. For the clinical patient case with a given portal field, the MR image-guided verification method provided an excellent match between features in both DRR-MRI and portal image. The accuracy of DRR-MRI was also examined by comparing it to the corresponding simulation image. The matching results indicated that the maximum deviation of anatomical features was less than 2.5 mm.

Adams et al. (2001) this study performed to assess 3-dimensional conformal radiotherapy (3D-CRT) and intensity-modulated radiotherapy (IMRT) techniques to see whether doses to critical structures could be reduced while maintaining planning target volume (PTV) coverage in patients receiving conventional radiotherapy (RT) for carcinoma of the maxillary sinus because of the risk of radiation-induced complications, particularly visual loss. Six patients who had recently received conventional RT for carcinoma of the maxillary sinus were studied. Conventional RT, 3D-CRT, and step-and-shoot IMRT plans were prepared using the same 2-field arrangement. The effect of reducing the number of

segments in the IMRT beams was investigated. 3D-CRT and IMRT reduced the brain and ipsilateral parotid gland doses compared with the conventional plans. IMRT reduced doses to both optic nerves for the contralateral optic nerve, 15-segment IMRT plans delivered an average maximal dose of 56.4 Gy (range 53.9–59.3) compared with 65.7 Gy (range 65.3–65.9) and 64.2 Gy (range 61.4–65.6) for conventional RT and 3D-CRT, respectively. IMRT also gave improved PTV homogeneity and improved coverage, with an average of 8.5% (range 7.0–11.7%) of the volume receiving <95% of the prescription dose (64 Gy) compared with 14.7% (range 14.1–15.9%) and 15.1% (range 14.4–16.1%) with conventional RT and 3D-CRT, respectively. Little difference was found between the 15 and 7-segment plans, but 5 segments resulted in a reduced minimal PTV dose. IMRT offers significant advantages over conventional RT and 3D-CRT techniques for treatment of maxillary sinus tumors. Good results can be obtained from 7 segments per beam without compromising the PTV coverage. This number of segments is practical for implementation in a busy RT department.

Prabhakar et al. (2008) the aim of the study was to show whether field-in-field (FIF) technique can be used to replace wedge filter in radiation treatment planning. The study was performed in cases where wedges are commonly used in radiotherapy treatment planning. Thirty patients with different malignancies who received radiotherapy were studied. This includes patients with malignancies of brain, head and neck, breast, upper and lower abdomen. All the patients underwent computed tomography scanning and the

datasets were transferred to the treatment planning system. Initially, wedge based planning was performed to achieve the best possible dose distribution inside the target volume with multileaf collimators (Plan1). Wedges were removed from a copy of the same plan and FIF plan was generated (Plan2). The two plans were then evaluated and compared for mean dose, maximum dose, median dose, doses to 2% (D2) and 98% (D98) of the target volume, volume receiving greater than 107% of the prescribed dose (V>107%), volume receiving less than 95% of the prescribed dose (V<95%), conformality index (CI) and total monitor units. FIF gives equivalent dosimetric results as wedge based treatment planning. It is better than wedge planning in terms of maximum dose, D2, V>107% and CI for most of the sites with statistically significant reduction in monitor units. FIF results in better dose distribution in terms of homogeneity in most of the sites. It is feasible to replace wedge filter with FIF in radiotherapy treatment planning.

Zaghloul et al. (2010) they assessed the accuracy of radiotherapy set-up using an electronic portal imaging device (EPID) versus megavoltage cone beam computed tomography (MV-CBCT) in pediatric patients. In total, 204 pairs of EPID and MV-CBCT were carried out for 72 patients in the first 3 treatment days and weekly thereafter. For the whole group, the mean systematic EPID set-up errors were 1.8 (±1.7), 1.6 (±1.3), 1.4 (±1.5) mm and 2.3 (±1.7), 1.6 (±1.3), 2.4 (±1.6) mm for MV-CBCT in the longitudinal, lateral and vertical directions, respectively, whereas the mean EPID random errors were 2.0 (±1.7), 1.4 (±1.5), 1.2 (±1.6) and 1.9 (±1.5), 1.5 (±1.3), 2.1 (±1.7) mm for MV-CBCT

in the longitudinal, lateral and vertical directions, respectively. For systematic errors of head and neck patients, there was a statistically significant difference in the lateral and vertical directions (P = 0.027, 0.003), whereas in the non-head and neck patients there was a statistically significant difference in the lateral direction only (P = 0.031). In head and neck patients, the mean random errors were significantly different in the vertical and lateral directions, whereas in non-head and neck patients, they were significantly different in the vertical direction only. The larger values alternate between the two modalities. The systematic and random errors (detected by EPID and MV-CBCT) were significantly correlated in almost all direction in all tumour sites.The comparison between set-up error in EPID and MV-CBCT was not in favour of any of the two modalities. However, the two modalities were strongly correlated but fairly agreed and the differences between the shifts reported were small and hardly influenced the recommended planning target volume margin.

Hurkmans et al. (2001) this review was used to verify the set-up error by means of portal imaging, they firstly define the various types of set-up errors using a consistent nomenclature. Next, the results of a large number of studies regarding patient set-up verification are presented for treatments of patients with head and neck, prostate, pelvis, lung and breast cancer, as well as for mantle field/total body treatments. This review focuses on the more recent studies in order to assess the criteria for good clinical practice in patient positioning. The reported set-up accuracy varies widely, depending on the

treatment site, method of immobilization and institution. The standard deviation (1 SD, mm) of the systematic and random errors for currently applied treatment techniques, separately measured along the three principle axes, ranges from 1.6–4.6 and 1.1–2.5 (head and neck), 1.0–3.8 and 1.2–3.5 (prostate), 1.1–4.7 and 1.1–4.9 (pelvis), 1.8–5.1 and 2.2–5.4 (lung), and 1.0–4.7 and 1.7–14.4 (breast), respectively. Recommendations for procedures to quantify, report and reduce patient set-up errors are given based on the studies described in this review. Using these recommendations, the systematic and random set-up errors that can be achieved in routine clinical practice can be less than 2.0 mm (1 SD) for head and neck, 2.5 mm (1 SD) for prostate, 3.0 mm (1 SD) for general pelvic and 3.5 mm (1 SD) for lung cancer treatment techniques.

Tsai et al. (1996) they used to develop and implement a non-invasive immobilization system guided by a dedicated quality assurance (QA) program for dynamic intensity-modulated radiotherapy (IMRT) of intracranial and head and neck disease, with IMRT delivered using the NOMOS Corporation's Peacock System and MIMiC collimator.

Thermoplastic face masks are combined with cradle-shaped polyurethane foaming agents and a dedicated quality assurance program to create a customized headholder system (CHS). Plastic shrinkage was studied to understand its effect on immobilization. Fiducial points for computerized tomography (CT) are obtained by placing multiple dabs of barium paste on mask surfaces at intersections of laser projections used for patient positioning. Fiducial lines are drawn on the cradle along laser projections aligned with nasal surfaces.

Lateral CT topograms are annotated with a crosshair indicating the origin of the treatment planning and delivery coordinate system, and with lines delineating the projections of superior-inferior field borders of the linear accelerator's secondary collimators, or with those of the fully open MIMiC. Port films exposed with and without the MIMiC are compared to annotated topograms to measure positional variance (PV) in superior-inferior (SI), right-left (RL), and anterior posterior (AP) directions. MIMiC vane patterns superposed on port films are applied to verify planned patterns. A 12-patient study of PV was performed by analyzing positions of 10 anatomic points on repeat CT topograms, plotting histograms of PV, and determining average PV. A 1.5 ± 0.3 mm SD shrinkage per 70 cm of thermoplastic was observed over 24 h. Average PV of 1.0 ± 0.8, 1.2 ± 1.1, and 1.3 ± 0.8 mm were measured in SI, AP, and RL directions, respectively. Lateral port films exposed with and without the MIMiC showed PV of 0.2 ± 1.3 and 0.8 ± 2.2 mm in AP and SI directions. Vane patterns superimposed on port films consistently verified the planned patterns. The CHS provided adequately reproducible immobilization for dynamic IMRT, and may be applicable to decrease PV for other cranial and head and neck external beam radiation therapy.

Mackie et al. (2001) they describe how helical tomotherapy compares with the image-guided practices being developed for conventional radiotherapy. Image guidance is beginning to be the fundamental basis for radiotherapy planning, delivery, and verification. Radiotherapy planning requires more precision in the extension and localization of disease.

When greater precision is not possible, conformal avoidance methodology may be indicated whereby the margin of disease extension is generous, except where sensitive normal tissues exist. Radiotherapy delivery requires better precision in the definition of treatment volume, on a daily basis if necessary. Helical tomotherapy has been designed to use CT imaging technology to plan, deliver, and verify that the delivery has been carried out as planned. The image-guided processes of helical tomotherapy that enable this goal are described. Image-guided precision conformal radiotherapy can be used as a tool to treat the tumor yet spare critical structures. Helical tomotherapy has been designed from the ground up as an integrated image-guided intensity-modulated radiotherapy system and allows new verification processes based on megavoltage CT images to be implemented.

Kadkhoda et al. (2008) the aim of this treatment planning study was to investigate the potential advantages of intensity-modulated (IM) proton therapy (IMPT) compared with IM photon therapy (IMRT) in nasopharyngeal carcinoma (NPC). Eight NPC patients were chosen. The dose prescriptions in cobalt Gray equivalent (Gy_E) for gross tumor volumes of the primary tumor (GTV-T), planning target volumes of GTV-T and metastatic (PTV-TN) and elective (PTV-N) lymph node stations were 72.6 Gy_E, 66 Gy_E, and 52.8 Gy_E, respectively. For each patient, nine coplanar fields IMRT with step-and-shoot technique and 3D spot-scanned three coplanar fields IMPT plans were prepared. Both modalities were planned in 33 fractions to be delivered with a simultaneous integrated boost technique. IMPT plans significantly improved the tumor coverage and conformation ($P <$

0.05) and they reduced the averaged mean dose to several organs at risk (OARs) by a factor of 2–3. The low-to-medium dose volumes (0.33–13.2 Gy_E) were more than doubled by IMRT plans. In radiotherapy of NPC patients, three-field IMPT has greater potential than nine-field IMRT with respect to tumor coverage and reduction of the integral dose to OARs and non-specific normal tissues. The practicality of IMPT in NPC deserves further exploration when this technique becomes available on wider clinical scale.

Mackenzie et al. (2002) this study used an inverse treatment planning (ITP) module on a commercial treatment planning system (TPS ~Helax AB, Uppsala, Sweden) for an in-house clinical trial for treatment of nasopharyngeal cancer with contralateral parotid sparing. Intensity modulated radiation therapy (IMRT) fields are delivered by step and shoot multileaf collimator (MLC) with a DMLC enabled Varian (2300 CD) Varian Associates, Palo Alto, (CA). A series of testing procedures have been devised to quantify the modeling and delivery accuracy of routine clinical inverse planned IMRT using. Helax TMS and the Varian step and shoot MLC delivery option. Testing was done on specific aspects of the TPS modeling germane to DMLC. Measured relative dose factors head scatter plus phantom scatter for small MLC fields, normalized to a 10310 cm2 non-MLC field, were found to differ by 2–3% from the TPS values for the smallest of the fields tested. Relative distributions for small off axis fields were found to be in good agreement. Each IMRT field in an inverse plan is imported into a flat water tank plan and a ‘‘beam’s eye view’’ BEV! Dose distribution is generated. This is compared to the corresponding

measured BEV dose distribution. The IMRT verification process has also been performed using ananthr opomorphic phantom. Large clinical fields ~i.e., greater than 14.5 cm in the leaf direction caused difficulties due to a vendor specific machine restriction, and several techniques for dealing with these were examined. These techniques were the use of static stepping of closed junctions, the use of two separate IMRT fields for a given gantry angle, and restricting the overall maximum field size used. Results of the verification measurements for the first ten patients treated at this center reveal an average maximum dose per IMRT field delivered of 71.0 cGy, with a mean local deviation from the planned dose of 21.2 cGy and a standard deviation of 2.4 cGy.

Langmack et al. (2001) they used a new media (films and electronic portal imaging devices) and confirmed this by markedly increasing the quality of portal images. Images from these devices can then be used to verify a patient's treatment. Geometric verification requires the portal image to be registered with a reference image. Dosimetric verification requires the portal imager to be calibrated for dose. This review gives a brief overview of the current areas of interest in portal imaging: imaging theory; imaging media, film and electronic portal imaging devices; image registration; and dosimetry using these devices.

Chapter Three

Materials and Methods

3-1 Materials:-

This study will carry out using Co-60 teletherapy machine with average energy 1.25 and percentage depth dose at 10cm with d_{max} at 0.5cm, Tray factor 0.98 and maximum field size is 45*45cm^2 , X-ray films , conventional simulator, portal film cassette, virtual simulator.

3-1-1 Design of the study:

This study is an analytical study where the treatment field boundaries will be verified by the simulator films of filed boundaries and collimator rotation of the treatment by the simulated one.

3-1-2 The Study population:-

The study consisted of patients treated with radical external beam radiation therapy for brain, nasopharynx and maxillary antrum cancer; their age ranged between 15 to 85years. The study carried out in RICK from February 2015 up to May 2016.

3-1-3 Method of data collection (technique):

The data was collected firstly from the patient files, then in the simulator the patient lies supine in the most of cases , while in some brain cases they lies in a porn position, with neck extended using suitable head rest and thermoplastic shell for immopolaization.The simulation process then start in order to specify the treatment filde borders. After the simulator image taken, we follow the patient to the treatment session to take a portal treatment image .After thee image processed we compare it with the simulator one to make the verification that we aimed to.

3-1-4 Variables of the study:

The data of this study were collected using the following variables: Age, Gender, FS, GR, CR, SSD, Separation, Total dose, X-value, Y-value and EFP.

Case	Gender	Age(year)	X(cm)	Y(cm)	EFP(cm)	T.D(Gray)	G.R	C.R	SSD(cm)	Sep(cm)

3-1-5 **Method of data analysis:**

This data will analyze using an Excel Microsoft office program and SPSS 16.0 and storage in personal computer with password.

3-1-6 Ethical issues:

The researcher has an ethical approval from the Hospital and the radiotherapy department as well as consent from the patient.

Chapter Four

Result

This study was focus in verification of matching the axis dimension of the planning treatment (simulator) and radiotherapy film, relation between TD and EFP, links between TD and SSD, present pathologic staging and grade, which are presented in tables and figures.

Table 4-1 shows parameters of the study.

Value	Mean	Std.Deviation	Minimum	Maximum

Stage	2.44	1.053	1	4
Grade	2.14	4	3	2
Age	2.81	1.608	1	7
X-axis/Sim	11.49	5.49	5.5	21
Y-axis/Sim	11.30	4.18	5	20
EFP	2.81	1.04	1.4	4.5
Total Dose	45.90	13.83	20	87
Gantry Rotation	172.11	90.45	90	270
Rotation/Sim	72.03	113.7	0	347
SSD	78.09	8.82	71	94
Sep	7.30	5.95	1	14

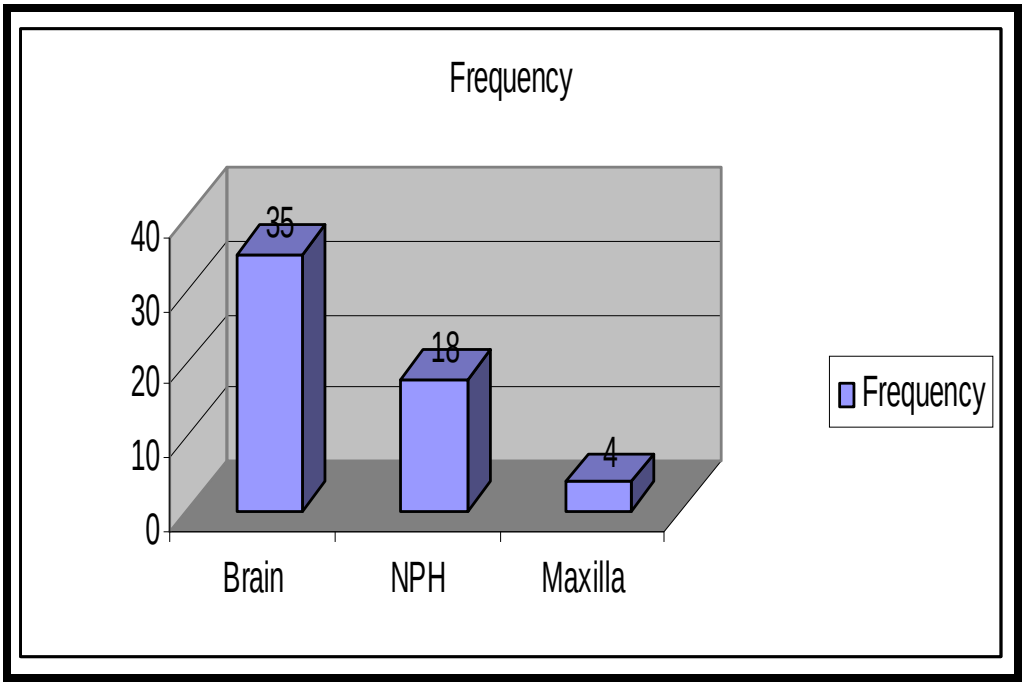

Figure 4-1 shows frequency of cases in this study.

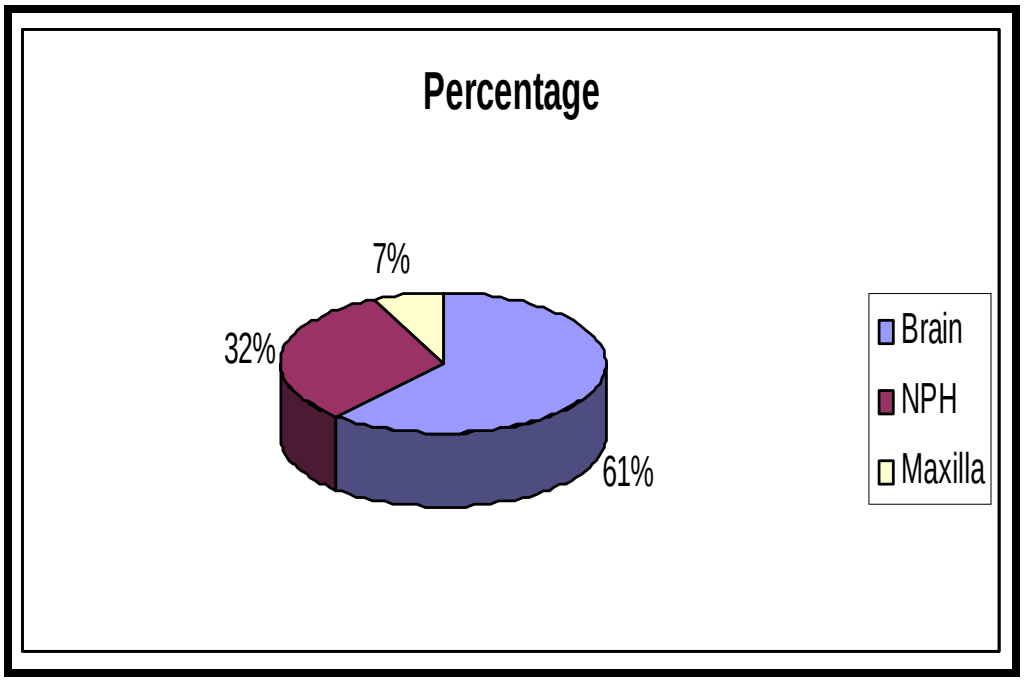

Figure 4-2 shows percentage of cases in this study

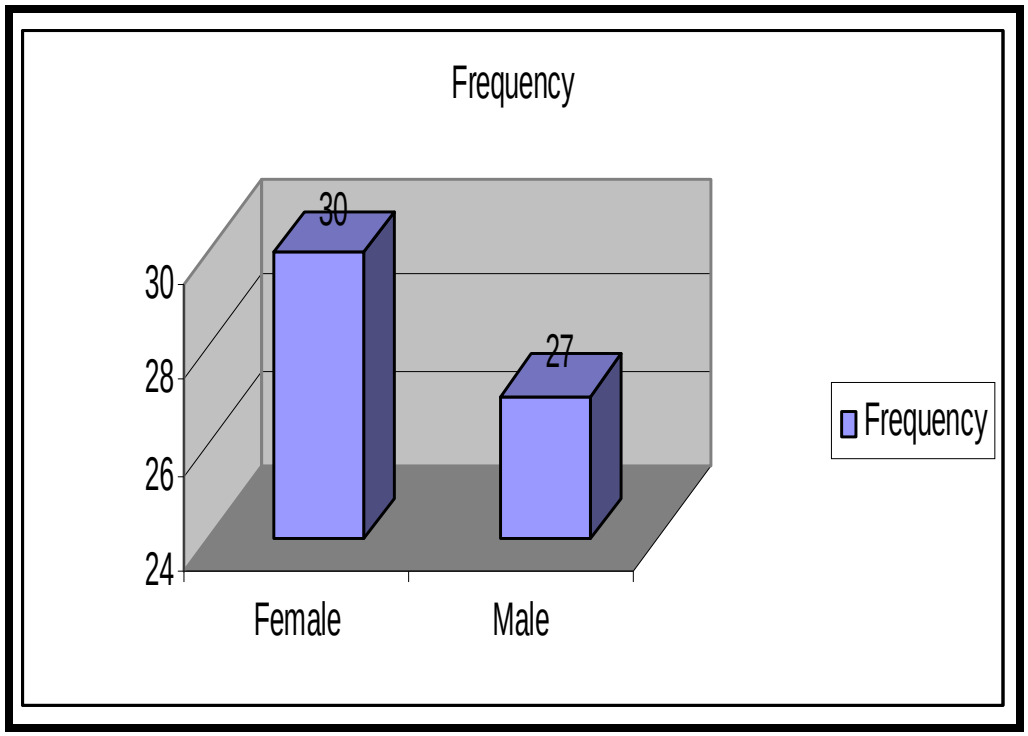

Figure 4-3 shows Male and Female frequency in this study.

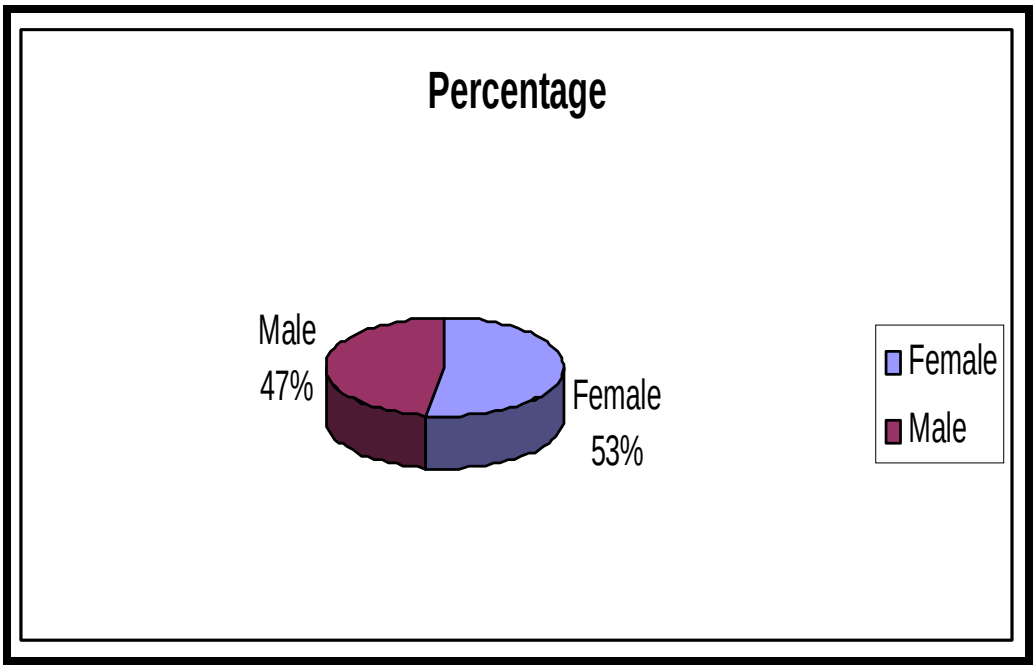

Figure 4-4 shows Male and Female percent in this study.

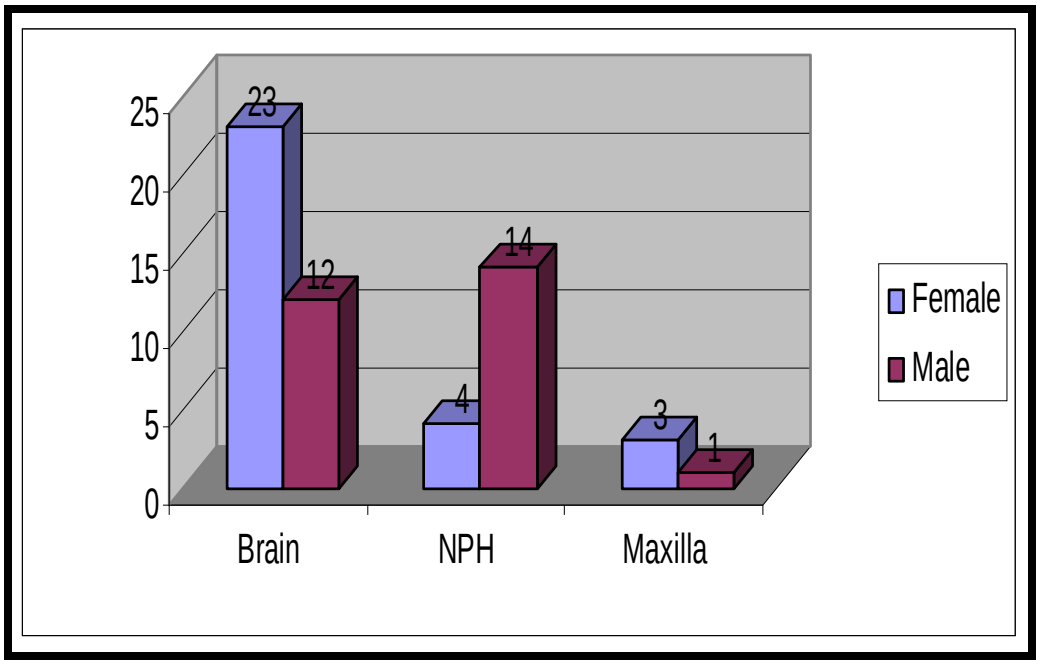

Figure 4-5 shows the gender presented in the study cases.

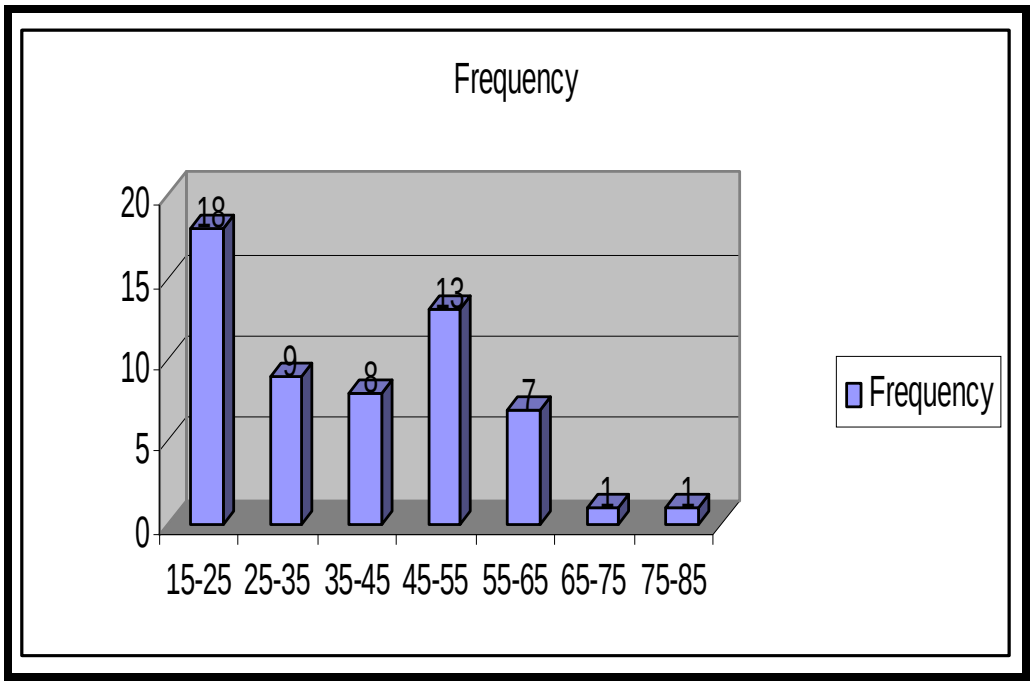

Figure 4-6 shows Age frequency in the study.

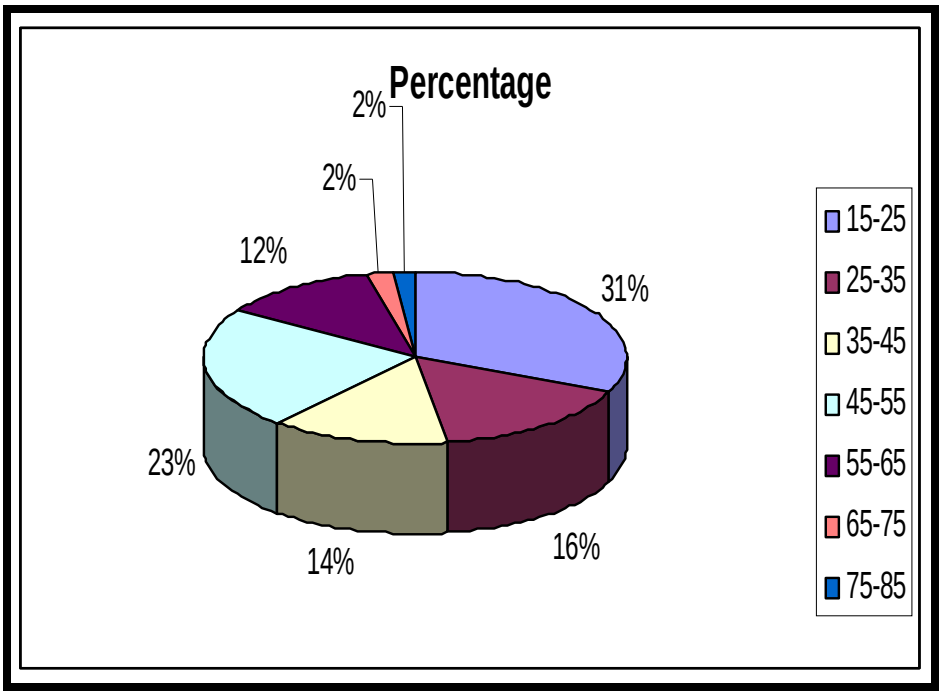

Figure 4-7 shows Age percent in the study.

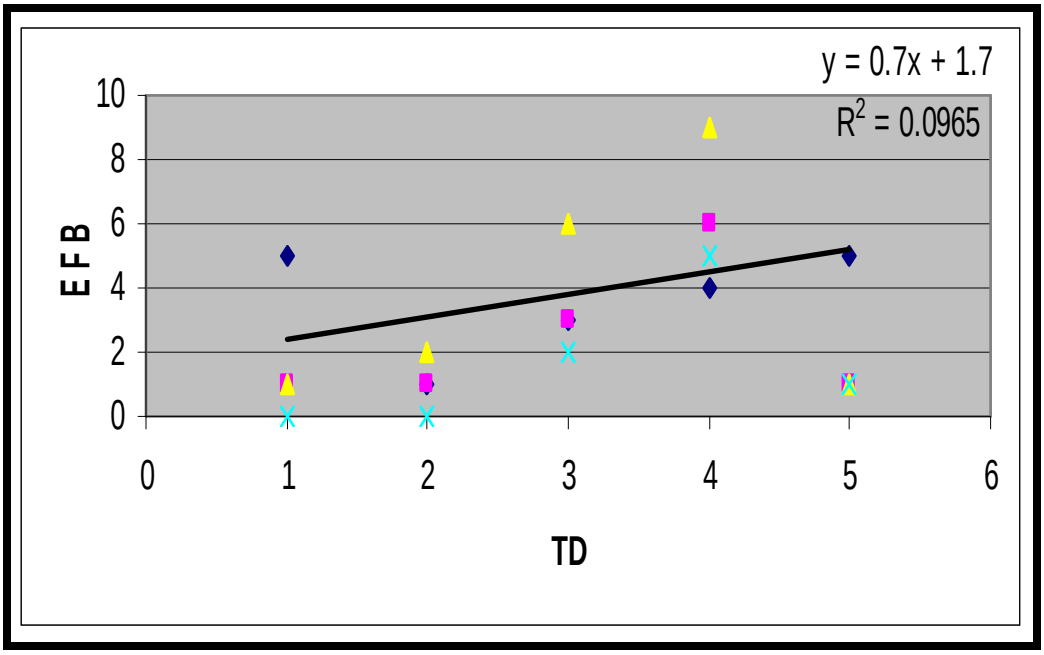

Figure 4-8 shows the relation between EFP and total given dose.

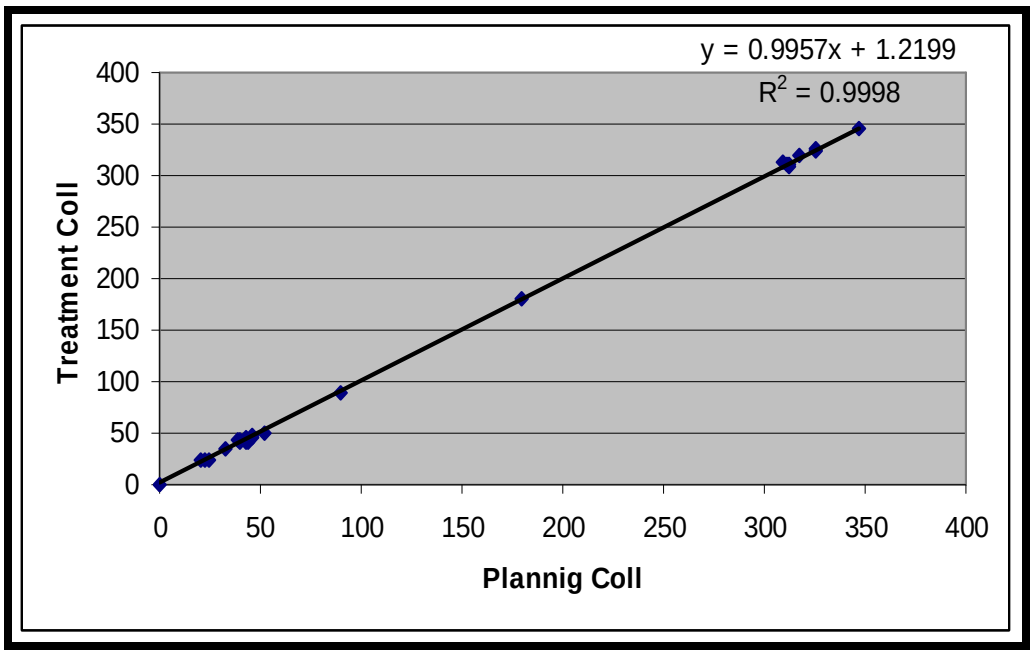

Figure 4-9 shows the relation between the Treatment & Planning collimator

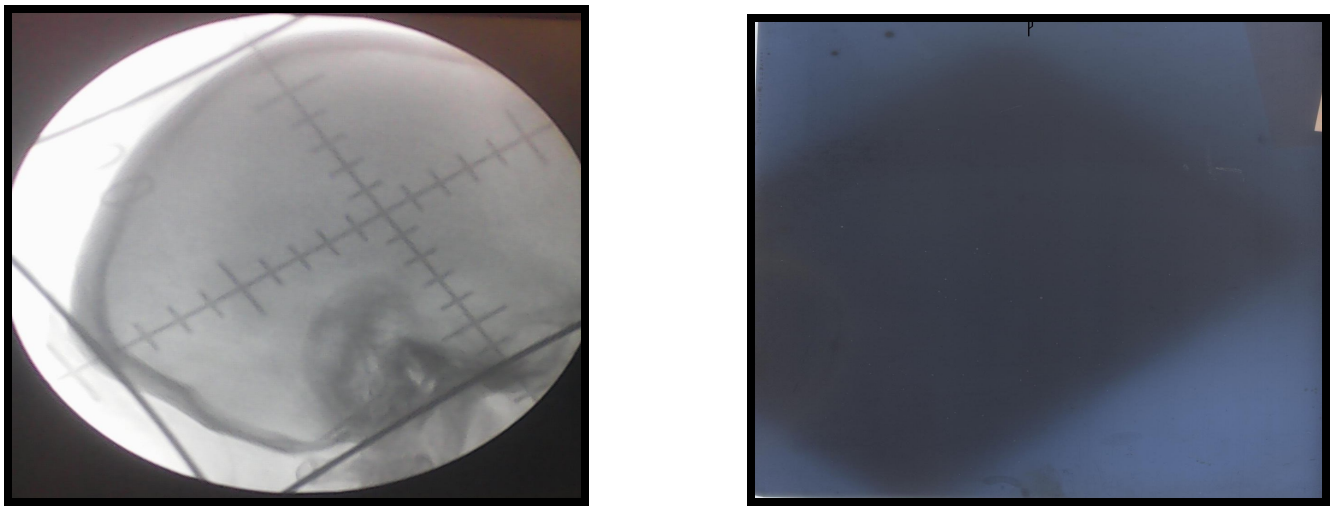

Figure 4-10 showed simulator filde size (19×15) & treatment filde size (20× 16).

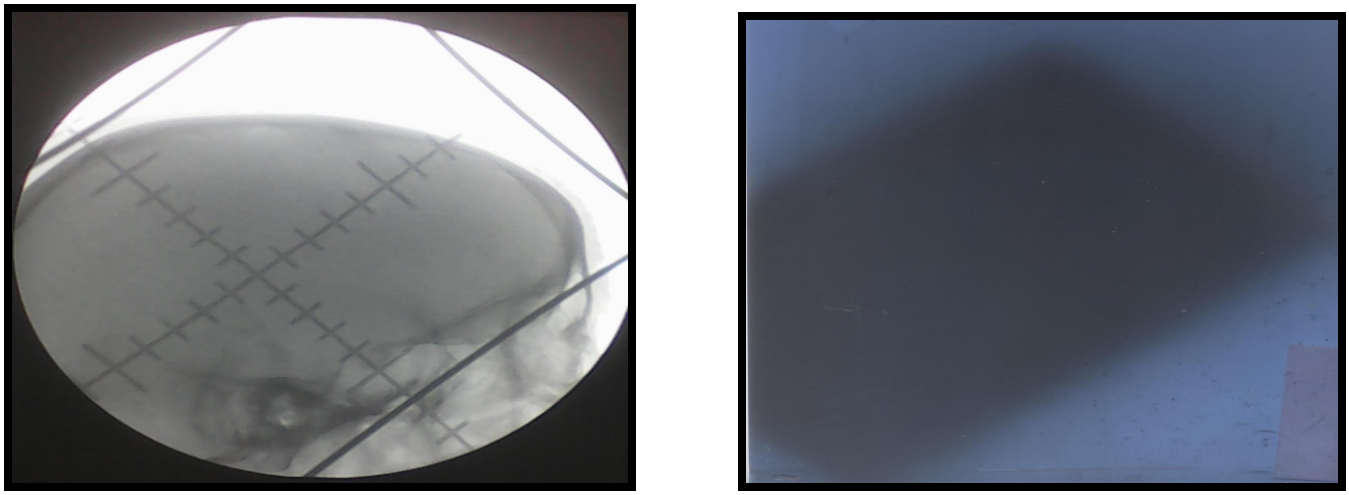

Figure 4-11 showed simulator filde size (19.5×13) & treatment filde size (18× 12.4).

Table 4-2 paired samples statistics between simulator and treatments images:

		Mean	N	Std. Deviation	Std. Error Mean
Pair 1	Sim X	9.68	25	4.643	.929
	Treat X	9.64	25	4.527	.905
Pair 2	Sim Y	9.00	25	3.452	.690
	Treat Y	8.96	25	3.259	.652

Table 4-3 Paired sample correlations between simulator and treatment image:

		N	*Correlation*	*Sig.*
Pair 1	*Sim X & Treat X*	*25*	*.982*	*.000*
Pair 2	*Sim Y & Treat Y*	*25*	*.989*	*.000*

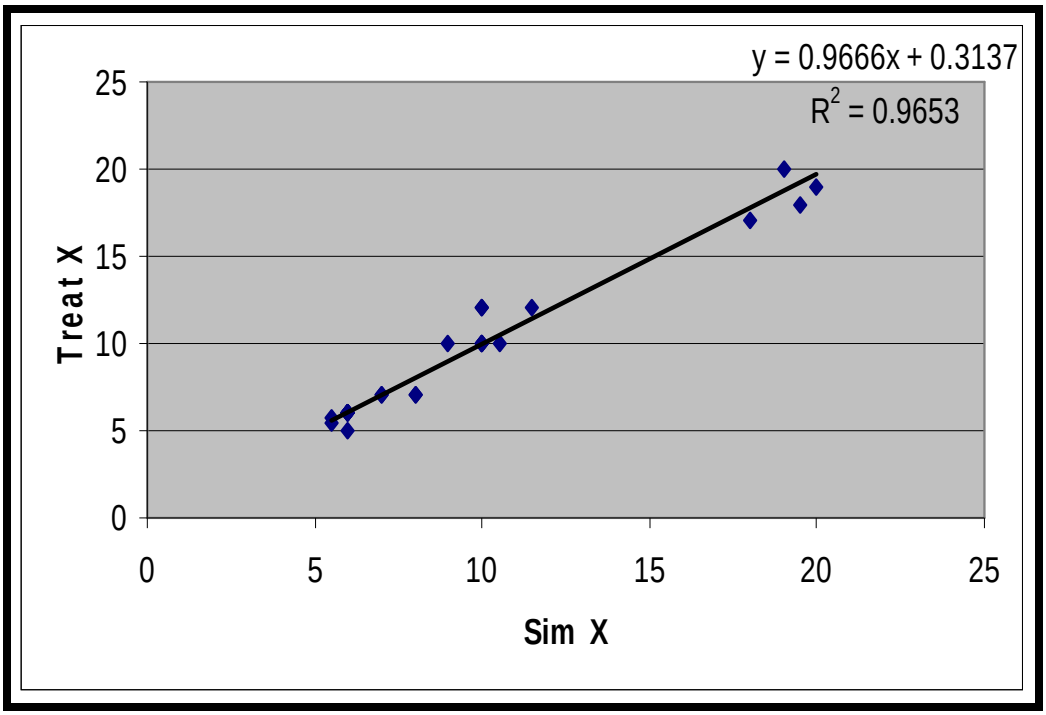

Figure 4—12 shows the relation between treatment & simulator X-axis.

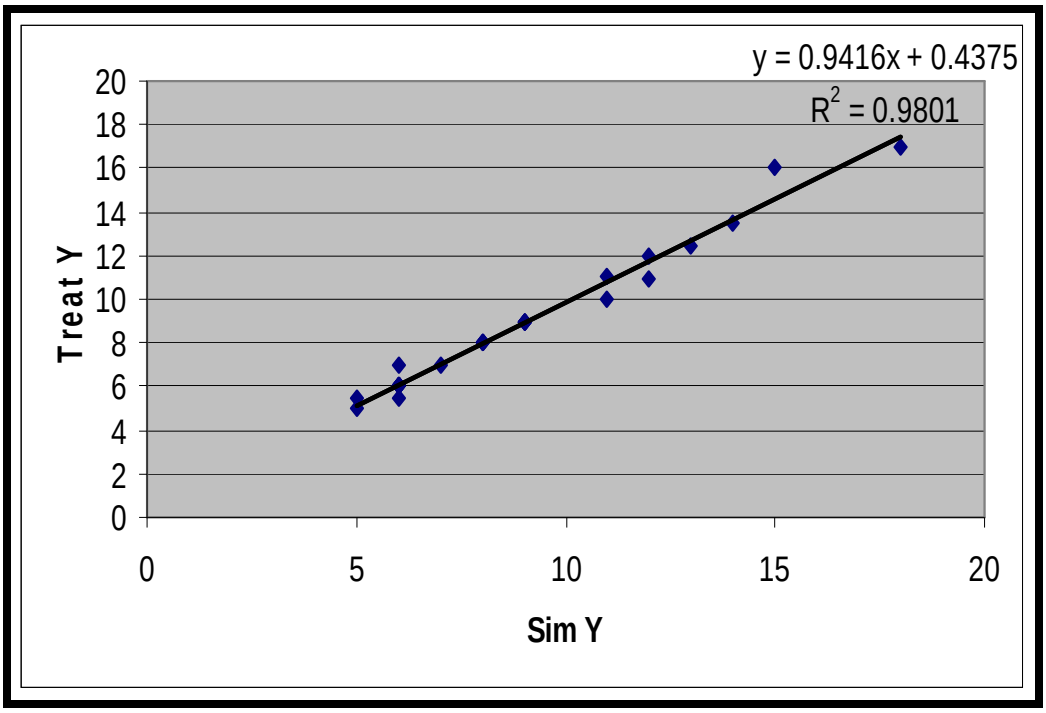

Figure 4—13 shows the relation between treatment & simulator Y-axis.

Chapter Five

5-1 Discussion:

This study was performed at RICK from February 2015 up to May 2016 and containing 57 patients. Table 4-1 show statistical parameters for all patients in means and SD. Figure 4-1 show frequency of cases were Brain represented 35 patients with percentage of 61.4% of all cases, 18 patients with nasopharyngeal cancer represented 31.58% per cent and 4 patients have a maxillary antrum tumor with 7.012% per cent as presented in figure 4-2. Most of the patients were female (30) while the remnant (27) were male, as represented in figure 4-3 with percentage of 52.63 & 47.37 respectively, as showed in figure 4-4.The

frequency of female cancers was 23-4-3 and 12-14-1 for male brain –nasopharynx and maxilla respectively as showed in figure 4-5.

Figure 4-6 showed the age groups represented in the study, were the patients with age group 15-25 was highest frequency and percentage of 31.5% ,then 45-55 with frequency of 13 and percentage of 22.8 % of all cases . While the lowest frequency was in 65-75 &75-85 with percentage of 17 % as in figure 4-7.

There is a linear relation ship between TD and EFP; it was found that the TD increased by 0.0965 Gray for each cm of EFB as presented in figure 4-8.

A linear correlation was represented in figure 4-9 between treated and simulated collimator rotation, were the correlation was very strong according to R^2=0.9998. A collimator rotation have an effective role in decreasing the dose to organ at risk, we were manipulated the angle to avoid the organ at risk over dose.

Using paired sample t-test show that the mean of simulator in X-axis 9.68±4.64 and for treatment film X-axis was 9.64±4.52, and for Y-axis for simulator 9±3.45 and for treatment film 8.96±3.25, as presented in table 4-2. It also showed that the correlation of x-axis for

simulator and treatment film 0.982 and of y-axis for the simulator and treatment film 0.989 as in table 4-3.

A linear regression results showed that the association between simulator and treatment film for X-axis was 0.96 per mm, and the rate of association for the simulator (X-Axis) and Treatment film (X-Axis) increases by 0.313 mm figure 4-12. Moreover, figure 4-13 represent the association between simulator and treatment film for Y-axis was 0.94 per mm, and the linear regression showed that the rate of association for the simulator (Y-Axis) and Treatment film (Y-Axis) increases by 0.437 mm.

Using t-test showed there are no significant differences between simulator and treatment film for X-axis and between simulator and treatment film for Y-axis.

5.2 Conclusion

Radiotherapy verification is the process that enables us to be certain we are treating the tumor volume as planned. In ensuring that the right radiation dose has been given to the right place, tow measures are needed, geometric and dosimetric verification.

The result show a linear relationship between total dose (T.D) and equivalent field parameter (EFB) were the dose does not change only the distribution does. A very strong linear correlation was represented according to R^2=0.9998 between treated and simulated

collimator rotation. A collimator rotation have an effective role in decreasing the dose to organ at risk, we were manipulated the angle to avoid the organ at risk over dose.

There is a significant liner relationship between X & Y values for simulator and treatment; we realize that while the values increase the error increase in order to. The result show that the mean of simulator in X-axis 9.68 ± 4.643 and for treatment film X-axis was 9.64 ± 4.527 and for Y-axis for simulator 9.00 ± 3.452 and for treatment film 8.96 ± 3.259. Using paired sample t-test showed that the correlation to x-axis for simulator and treatment film 0.982 and to y-axis for the simulator and treatment film 0.989. Using t-test show there is no significant differences between simulator and treatment film for X-axis and between simulator and treatment film for Y-axis.

The association between simulator and treatment film for X-axis was 0.96 mm/mm, and for Y-axis was 0.94 per mm for each mm.

Linear regression results showed that the rate of association for the simulator (X-Axis) and Treatment film (X-Axis) increases by 0.313 mm, and the rate of association for the simulator (Y-Axis) and Treatment film (Y-Axis) increases by 0.437 mm.

5.3 Recommendation

- Radiation delivery should be as accurate as possible to planned area to resects the tumors and avoid OAR irradiation by using effective patients immobilization devices in order to obtain good recovery, Portal film can be very beneficial for that purpose.
- Every radiotherapy treatment department must take geometrical and dosemtrical changes as a primary part of daily QC of radiotherapy procedure.

- Head and Neck consider to be the most area with sensitive fetal organs, thus we must shielding the critical organs such as lens, brain stem, spinal cord…..etc from scatter radiation in order to avoid exceeding the reference doses.
- As we used Methods of In field dose calculation, we must also invest Methods of out-field dose calculation especially in CO-60 which is consider a continuous irradiating source like day-methods, and Output factor of machine calculation, also we can use ionization champers and TLD….. etc as recurred.
- Nevertheless, Simulator can be an effective tool to obtain check film firstly then compared it with portal one.
- Portal imaging, with film or preferably with a real time imaging device, should be used routinely to verify patient setup relative to the therapy beam for external radiation therapy.

References

-American Cancer Society, 2010, Brain and Spinal Cord Tumors in Adults, Atlanta.

-Armstrong T, 2011, Central nervous system cancer, Cancer Nursing Principles and Practice, 7th Edition, Sudbury, MA: Jones and Bartlett. 49: pp. 1146-1187.

-Martini, F. H., Timmons, M. J., & Tallitsch, R. B. (2012). *Human Anatomy*. (7th Edition). San Francisco: Pearson Benjamin Cummings.

- Benjamin Cummings, 2006, Respiratory Syster PDF, Pearson Education, p. 1.

-Clinical Head and Neck and Functional Neuroscience Course Notes, 2008-2009, Uniformed Services University of the Health Sciences School of Medicine, Bethesda, Maryland

-Simkins Ph.D, 1943, Functional Anatomy OF The Eustachian Tube, Cleveland, Arch Otolaryngology, 38(5):476-484.

- Elsevier, 2008, Human Anatomy, Jacobs, page 209-210

- G.W, 2011, Maxillary sinus disease: diagnosis and treatment, *British Dental Journal* 210, 113 – 118.

- Fehrenbach and Herring, 2012, Illustrated Anatomy of the Head and Neck, Elsevier, page 67.

- Glenn E. Sheline PHD, MD, 2006, American Cancer Society's National Conference on Radiation Oncology Present Status and Future Potential, Volume pages 873–881, American Cancer Society, San Francisco, California.

- Sultanem K, Shu HK, Xia P, et al, 2000 , Radiat Oncol Biol Phys Int J, the University of California–San Francisco experience , p. 48:711–22,San Francisco.

- Eisbruch A, Ten Haken RK, Kim HM, Marsh LH, Ship J, 1999,Dose, volume, and function relationships in parotid salivary glands following conformal and intensity-modulated irradiation of head and neck cancer, Int J Radiat Oncol Biol Phys.;45:577–87.

- Ballivy , 2006, Curr Oncol; 13(3): 108–115, PMCID: PMC1891177._V. 13(3).

- Stratford J, Ball K, Henry AM, 2006, Radiotherapy treatment verification in the UK: an audit of practice in Clin Oncol.

- British Institute of Radiotherapy, 2001, Gaeometric uncertainties in Radiotherapy, London.

- Jaffrey D A, 2007, Image-guided radiation therapy, p: 243-244, Semin Radiation Oncology.

- VanHerk M, Remeijer P, Rassch C, Lebesque JV, Int J, 2000, the probability of correct target dosage, pag: 1121-1135, Radiation Oncology Biophysics.

- Bethesda, 1999, International Commission on Radiation Units and Measurement.

- UICC International Union against Cancer, 2002, p: 15–22.

- Chao KS, Deasy JO, Markman J, 2001, Int J Radiat Oncol Biol Phys.; p: 49:907–

- H. Huizenga, 1988, Radio therapeutic Institute, Department of Physics, 3075 EA Rotterdam, The Netherlands, Volume, Pages 181-187.

- Patchell RA, 1998, Postoperative radiotherapy in the treatment of single metastases to the brain: a randomized trial. JAMA; 280(17): 1485–1489. Pmid: 9809728 doi: 10.1001/jama.280.17.1485

- Clemens F. Hess Gottingen, 1995, Accuracy of field alignment in radiotherapy of head and neck cancer utilizing individualized face mask immobilization: a retrospective analysis of clinical practice, Published by Elsevier Ireland Ltd, Germany, Volume, Pages 69-72.

- Yin FF, Gao Q, Xie H, Nelson DF, Yu Y, Kwok WE, Totterman S, Schell MC, Rubin P, 1998, MR image-guided portal verification for brain treatment field , National Center for Biotechnology Information, Bethesda MD, Int J Radiat Oncol Biol Phys,USA.

- lizabeth J. Adams, M.Sc., 2001, International Journal of Radiation Oncology*Biology*Physics**,**Joint Department of Physics, Royal Marsden NHS Trust, Downs Road, Sutton, UK, Elsevier Science Inc, Volume 51, Issue 3, 1 November 2001, Pages 579–588.

- Prabhakar, R., Julka, P.K. & Rath, G.K. Australas, 2008, Medicine, Australia.

- M.S. Zaghloul, 2010, Oncology, Volume, December 2010, Pages 850–861**,** Radiation Oncology Department, Children's Cancer Hospital, Sayeda Zainab, The Royal College of Radiologists, Egypt, Cairo, Published by Elsevier Ltd.

- Coen W Hurkmans, 2001, Radiotherapy and Oncology **,**Volume 58, Issue 2, Pages 105–120 Ireland, Elsevier Science Ireland Ltd.

- Jen-San Tsai, 1996,International Journal of Radiation Oncology*Biology*Physics Volume 43, Issue 2, 15 January 1999, Pages 455–467, New England Medical Center, 750 Washington Street, Boston.

- Thomas Rockwell Mackie, 2003, International Journal of Radiation Oncology*Biology*Physics ,Volume 56, Issue 1, Pages 89–105, Madison, USA, Elsevier Science Inc.

- Yeh SA, 2005, Int J Radiat Oncol Biol Phys.; pag 62:672–679.

- Boyer AL, Antonuk L, Fenster A, van Herk M,2001 ,The British Journal of Radiology, Greetwell Road, Lincoln, UK.

- Meertens H, Munro P, et al, 1992, Med Phys.

Abbreviation

AP: Anterior posterior

BEV: Beam's eye view

BMI: Body mass index.

CHS: Customized headholder system

CI: Conformality index

CNS: central nervous system

CT: Computerized tomography

CTV: Clinical target volume

Ctvs: Clinical target volumes

CR: Collimator rotation.

3D-CRT: 3-Dimensional conformal radiotherapy

DD: Daily dose.

DRR-CT: Digitally reconstructed radiographs directly from computed tomography.

DRR-MRI: Digitally reconstructed radiographs directly from magnetic resonance images.

EBRT: External beam radiation therapy.

EDR2: Extended dose rate

EFP: Equivalent filed parameters (= $(a \times b) \div 2 (a + b)$).

EPID: Electronic portal imaging device

FIF: Field-in-field

FS: Filde size.

g –index: gamma-index

GR: Gantry rotation.

GTV: Gross tumour volume

GTV-T: Gross tumor volumes of the primary tumor

Gy_E: Gray equivalent

H: Hight.

ICRU: International Commission on Radiation Units and Measurement.

IM: Intensity-modulated

IMPT: Intensity-modulated proton therapy

IMRT: Intensity-modulated radiotherapy

ITP: Inverse treatment planning

ITV: Internal target volume

MLC: Multileaf collimator

MV-CBCT: Megavoltage cone beam computed tomography

NPC: Nasopharyngeal carcinoma

OAR: Organs at risk

PNS: Peripheral nervous system

PRV: planning organ-at-risk volume

PV: Positional variance

PTV: Planning target volume

PTV-N: Planning target volumes of GTV and elective

PTV-TN: Planning target volumes of GTV-T and metastatic

QA: Quality Assurance

RICK: Radiation and Isotopes Center Khartoum.

RL: Right-left

RT: Radiotherapy

SAD: Source to axis distance

Sep: Separation.

SI: Superior-inferior

SD: Stander deviation**.**

SSD: Surrfec to skin distance.

SSD: Source to surface distance

TBI: Total body irradiation

TD: Total dose.

TEV: Target eye view

TPS: Treatment planning system

W: Wight.

X: Width of the filde.

Y: Length of the filde.

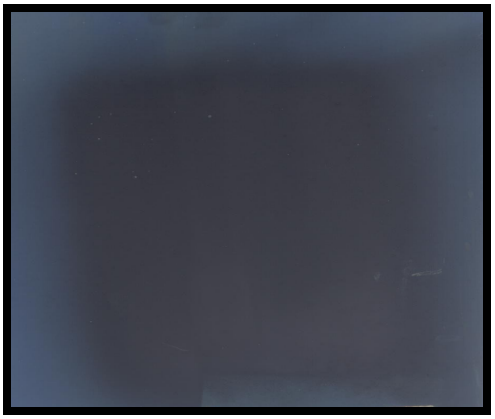

Figure (4-16) shows simulator filde size (8ˣ12) & treatment filde size (7ˣ12).

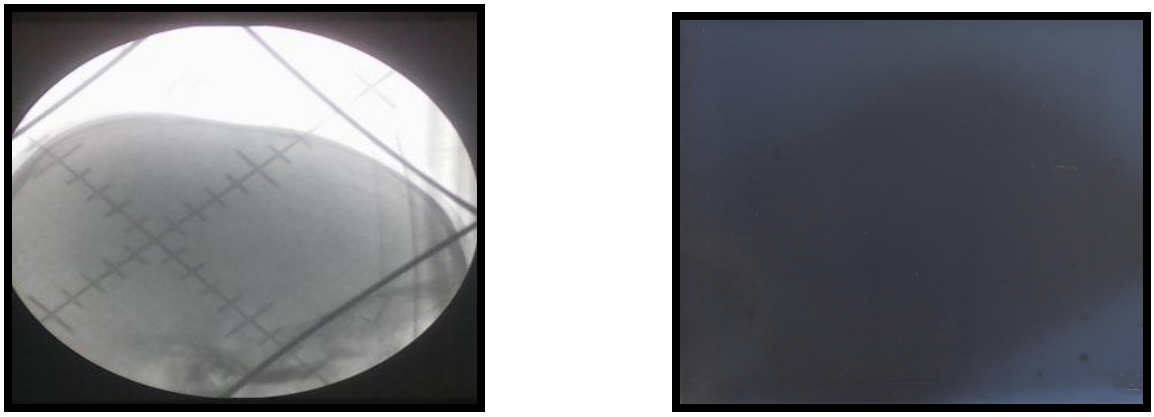

Figure (4-17) shows simulator filde size (18ˣ14) & treatment filde size (17ˣ13.5).

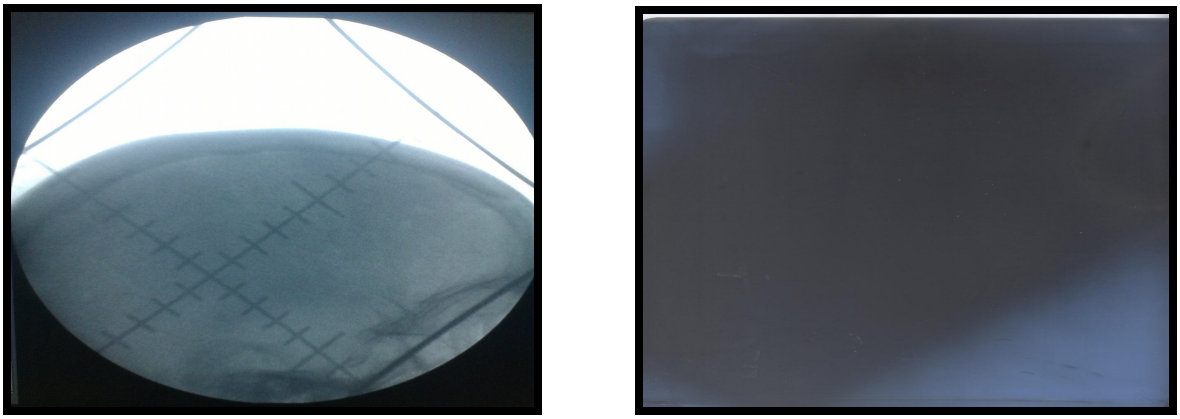

Figure (4-18) shows simulator filde size (20ˣ12) & treatment filde size (19ˣ10.9).

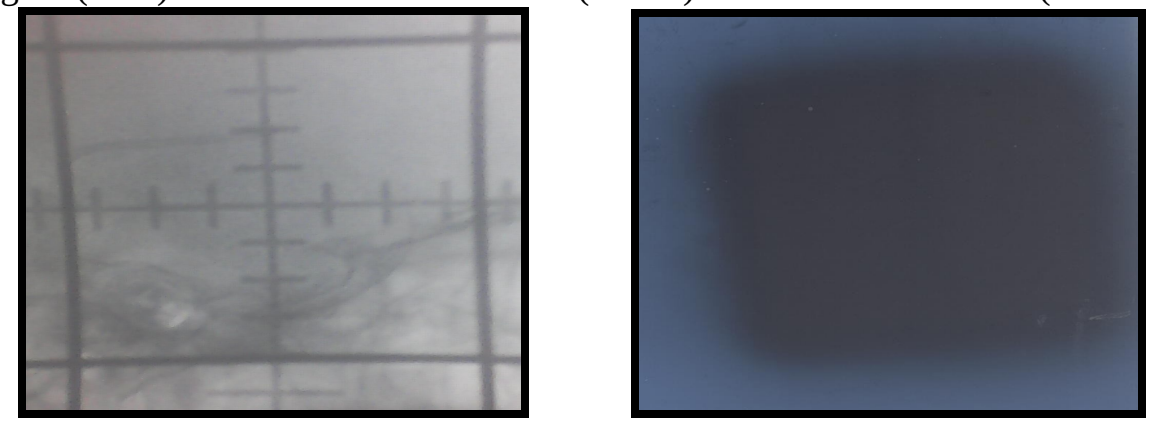

Figure (4-19) shows simulator filde size (7ˣ8) & treatment filde size (7ˣ8).

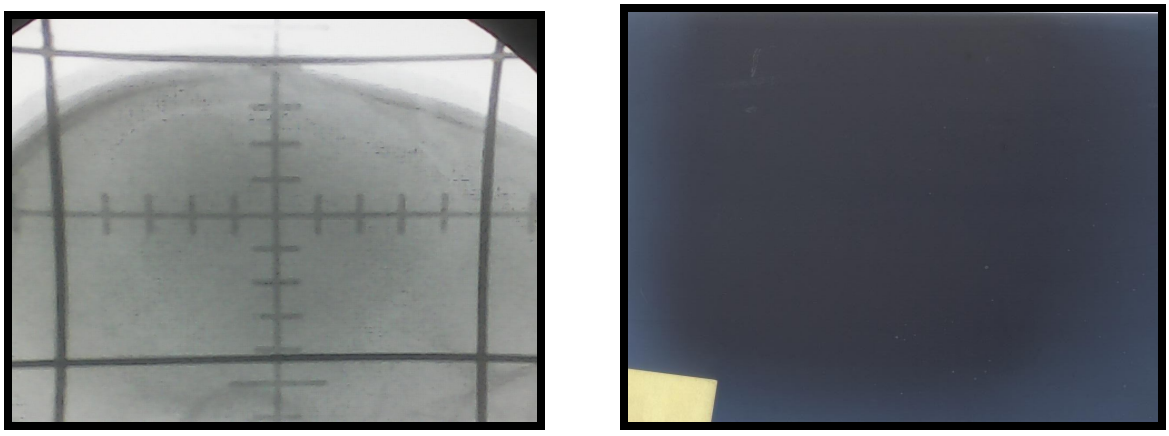

Figure (4-20) shows simulator filde size (10ˣ9) & treatment filde size (12ˣ9).

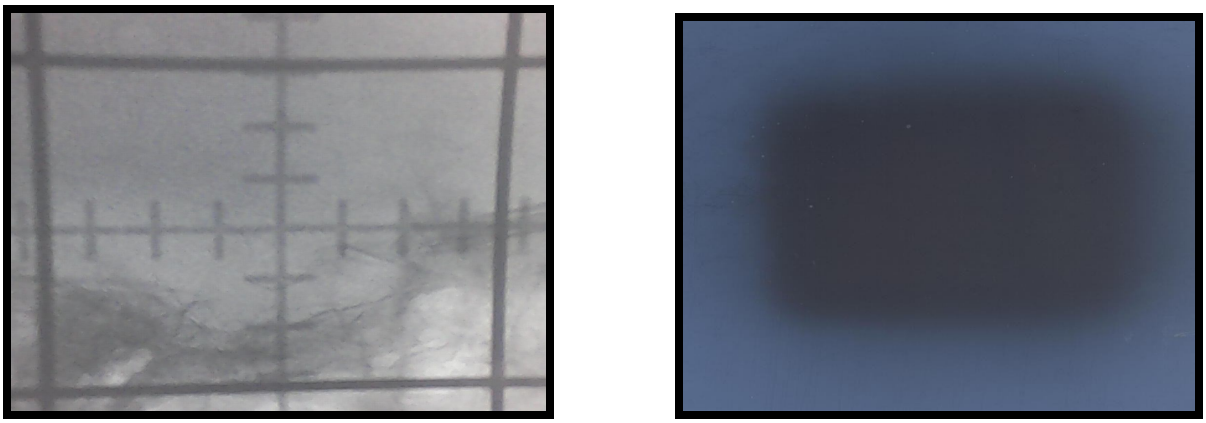

Figure (4-21) shows simulator filde size (7ˣ6) & treatment filde size (7ˣ7)

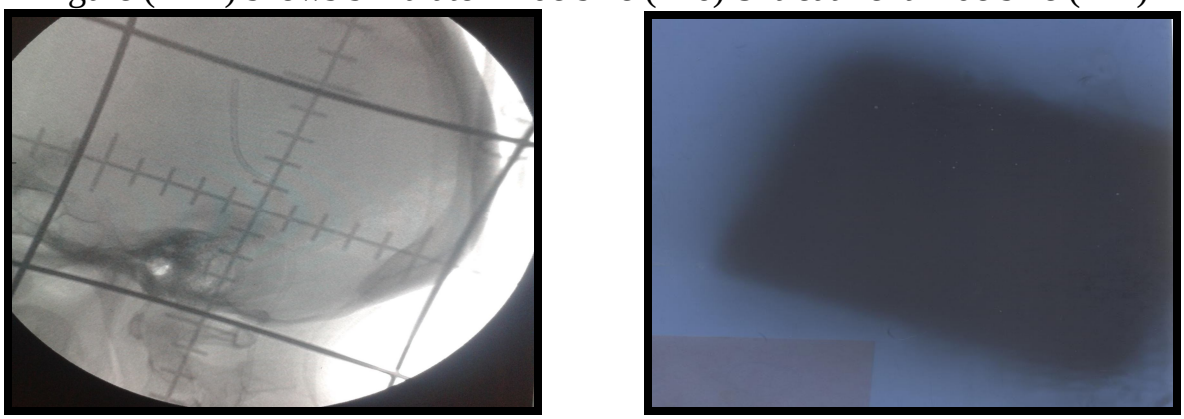

Figure (4-22) shows simulator filde size (11.5ˣ9) & treatment filde size (12ˣ9).

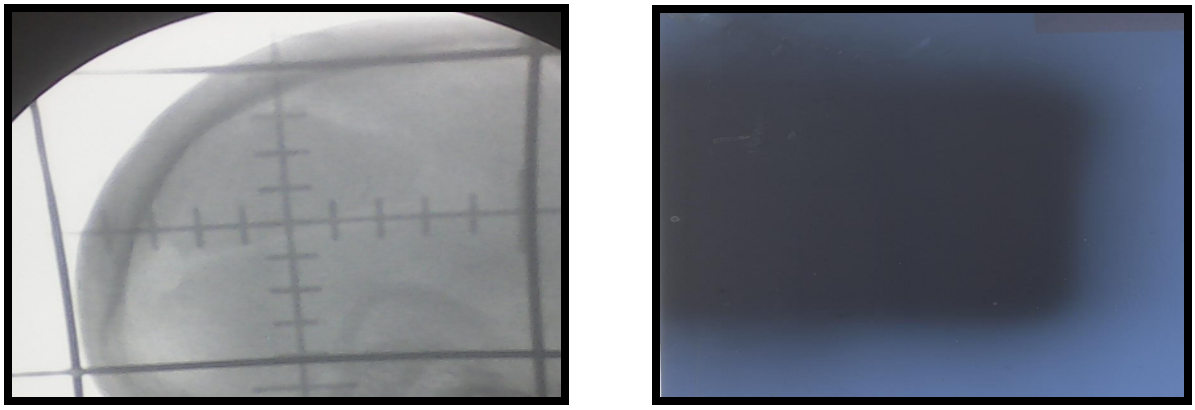

Figure (4-23) shows simulator filde size (10ˣ8) & treatment filde size (10ˣ8).

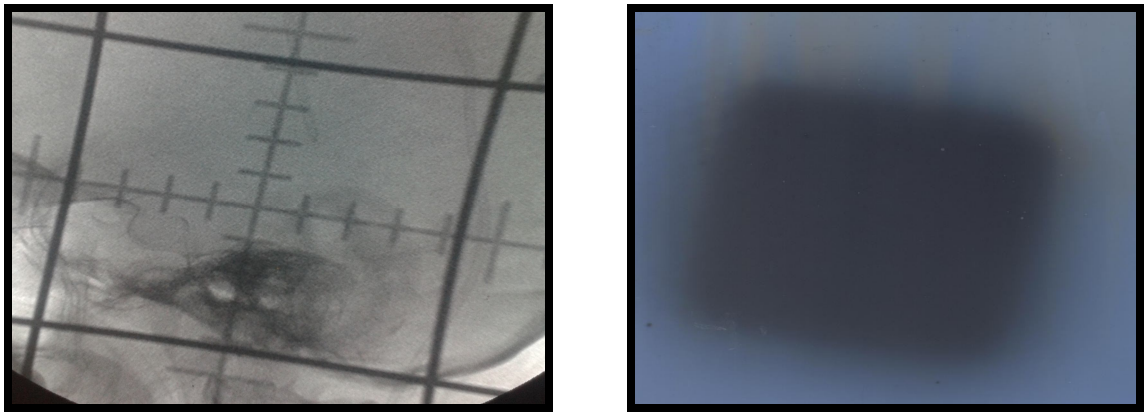

Figure (4-24) shows simulator filde size (8ˣ8) & treatment filde size (7ˣ8).

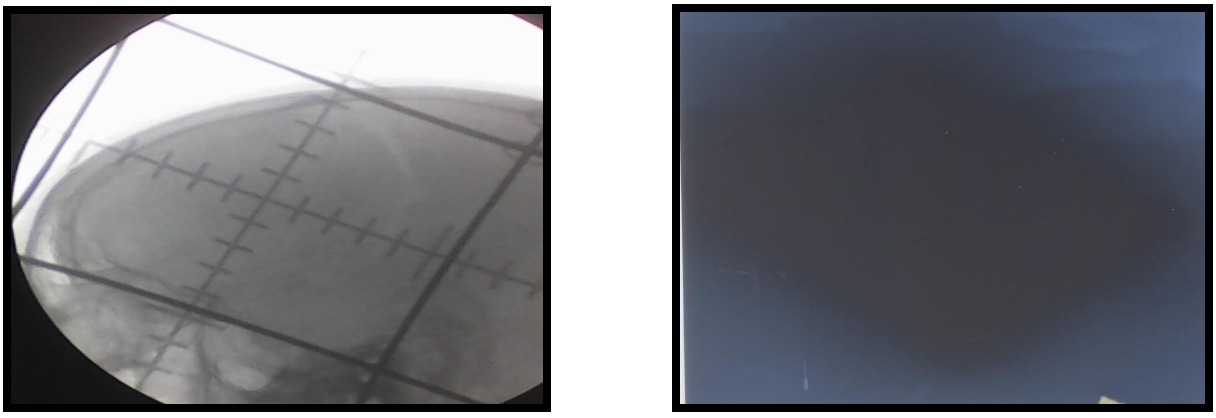

Figure (4-25) shows simulator filde size (10.5ˣ9) & treatment filde size (10ˣ9).

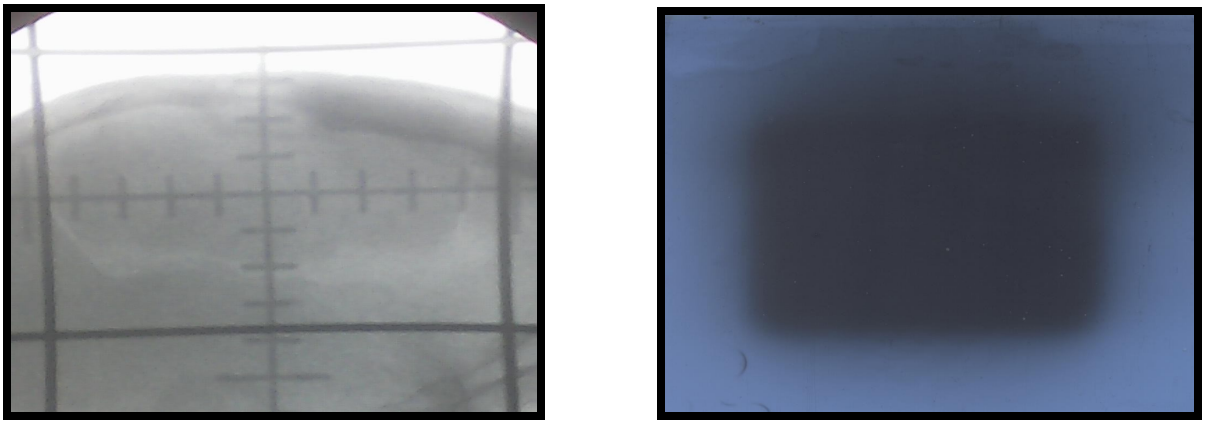

Figure (4-26) shows simulator filde size (9ˣ7) & treatment filde size (10ˣ7).

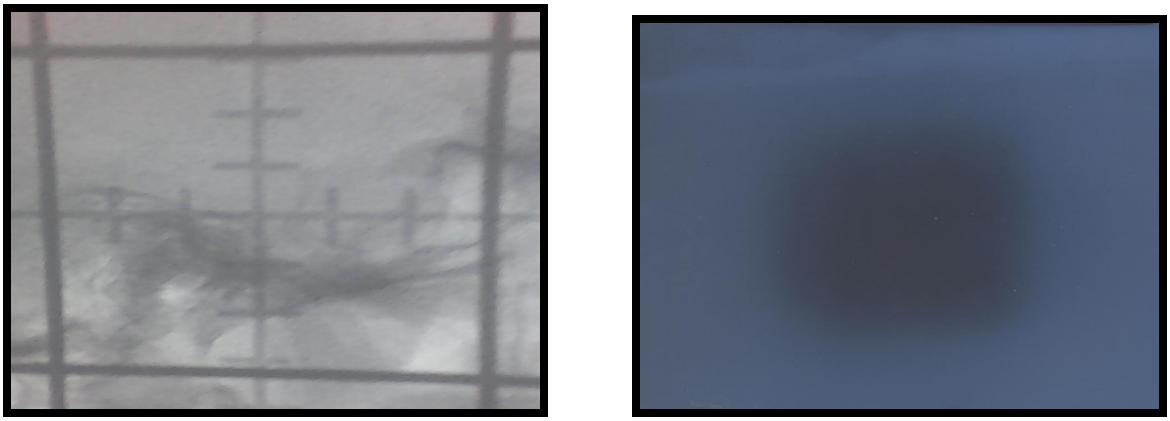

Figure (4-27) shows simulator filde size (6ˣ6) & treatment filde size (6ˣ6).

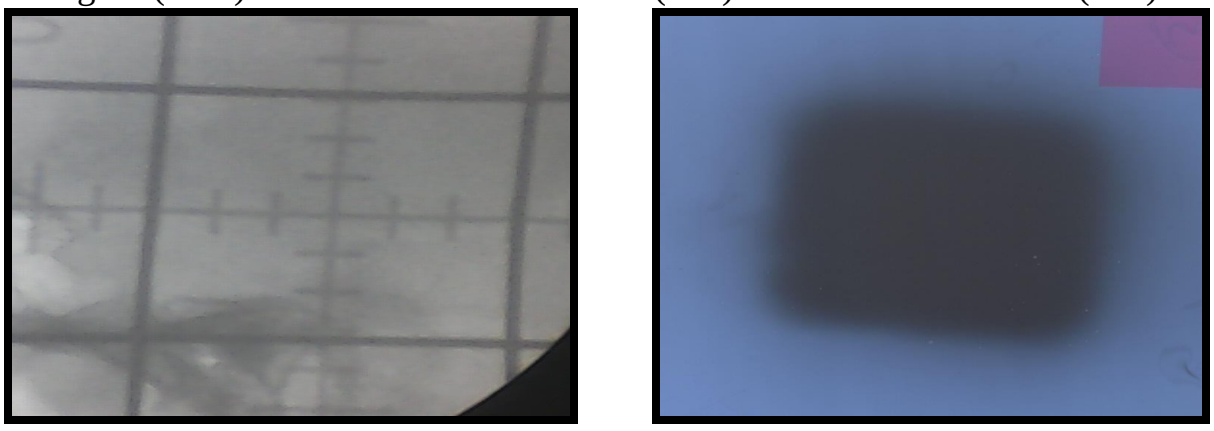

Figure (4-28) shows simulator filde size (6ˣ6) & treatment filde size (6ˣ6).

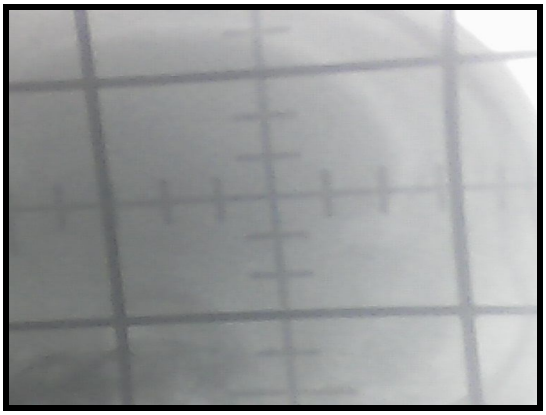

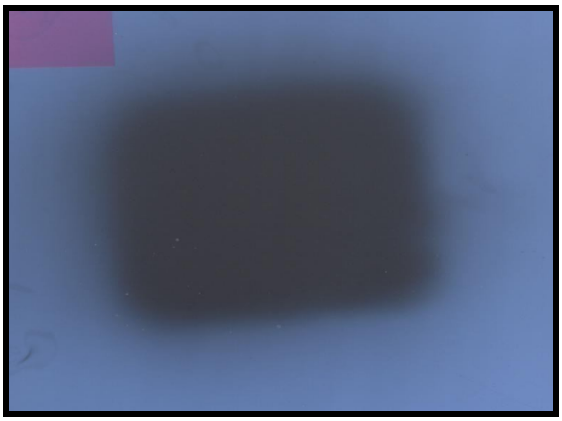

Figure (4-29) shows simulator filde size (6ˣ6) & treatment filde size (6ˣ6).

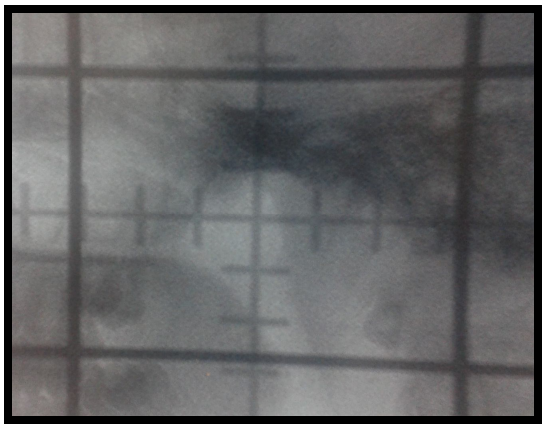

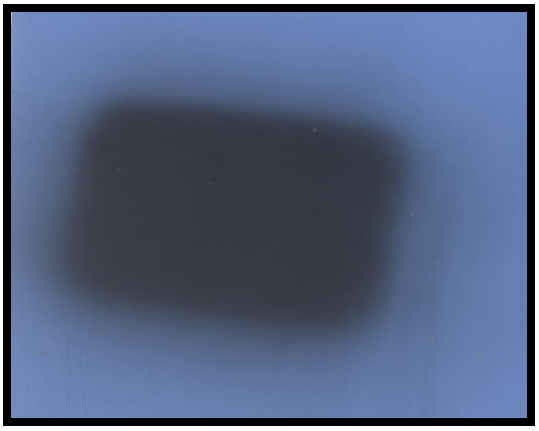

Figure (4-30) shows simulator filde size (5.5ˣ6) & treatment filde size (5.5ˣ5.5).

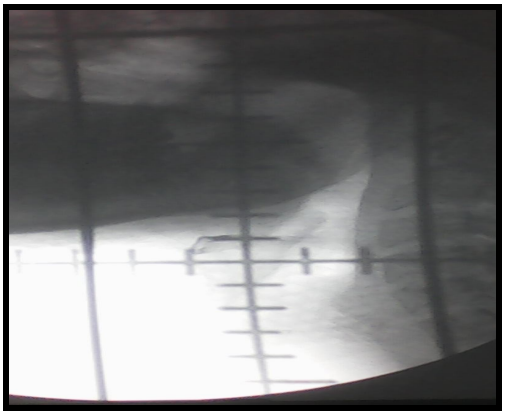

Figure (4-31) shows simulator filde size (5.5ˣ18) & treatment filde size (5.8ˣ17).

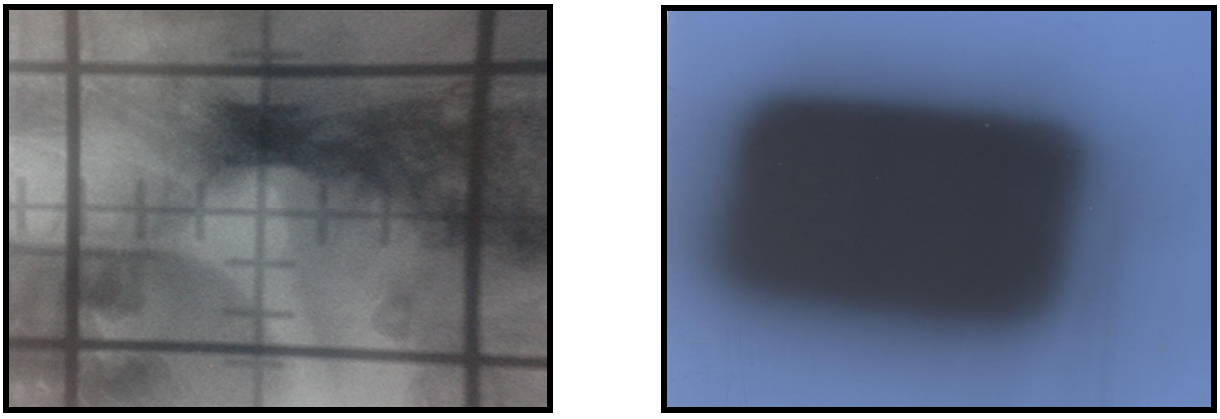

Figure (4-32) shows simulator filde size (6ˣ5) & treatment filde size (6ˣ5).

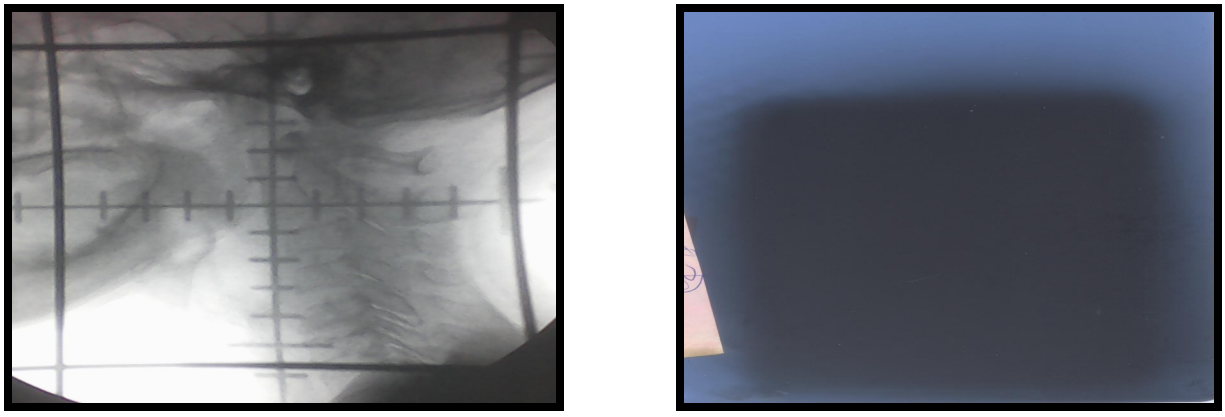

Figure (4-33) shows simulator filde size (10ˣ11) & treatment filde size (10ˣ11).

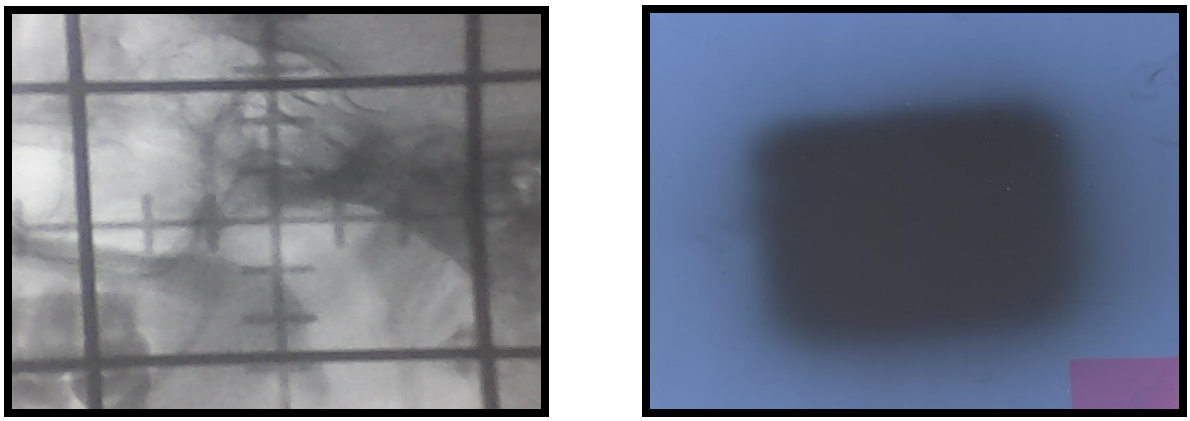

Figure (4-34) shows simulator filde size (6ˣ6) & treatment filde size (6ˣ6).

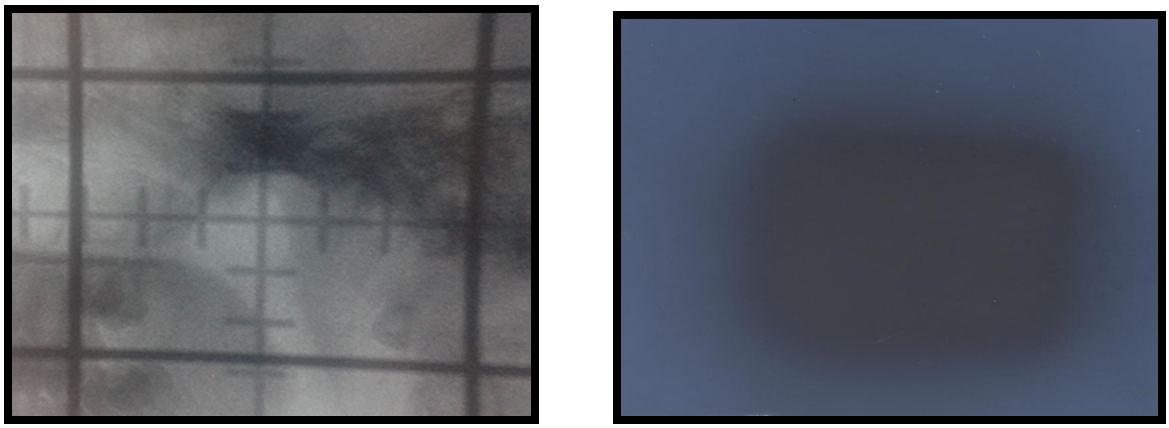

Figure (4-35) shows simulator filde size (6ˣ5) & treatment filde size (6ˣ5.5).

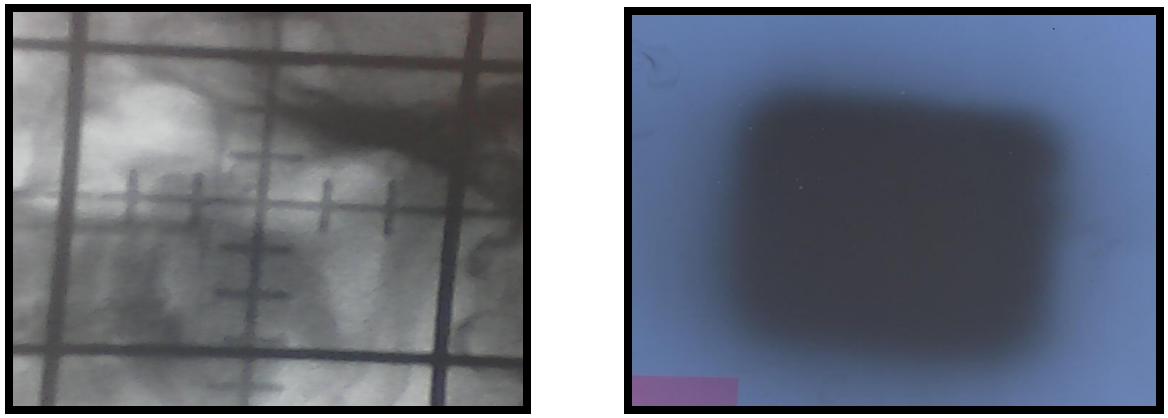

Figure (4-36) shows simulator filde size (6ˣ6) & treatment filde size (5ˣ6).

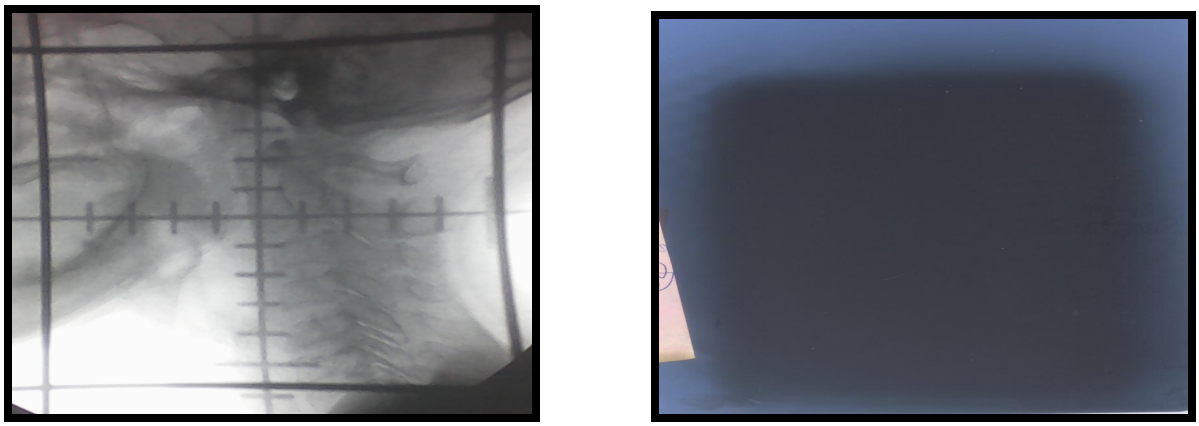

Figure (4-37) shows simulator filde size (10 x 11) & treatment filde size (10 x 10).